Annales Academiæ Scientiarum Fennicæ
Mathematica
Volumen 42, 2017, 771–797

SOBOLEV HOMEOMORPHISMS IN $W^{1,k}$ AND THE LUSIN'S CONDITION (N) ON k-DIMENSIONAL SUBSPACES

Stanislav Hencl and Aapo Kauranen

Charles University, Department of Mathematical Analysis
Sokolovská 83, 186 00 Prague 8, Czech Republic; hencl@karlin.mff.cuni.cz

aapo.p.kauranen@gmail.com

Abstract. We construct a Sobolev homeomorphisms $F \in W^{1,2}((0,1)^4, \mathbf{R}^4)$ which fails the 2-dimensional Lusin's condition on $\mathcal{H}^2$-positively many hyperplanes, i.e. there exists $\mathcal{C}_1 \subset [0,1]^2$ with $\mathcal{H}^2(\mathcal{C}_1) > 0$, such that for each $(z,w) \in \mathcal{C}_1$ there is a set $A_{(z,w)} \subset [0,1]^2$ with $\mathcal{H}^2(A_{(z,w)}) = 0$ and $\mathcal{H}^2\big(F(A_{(z,w)} \times \{(z,w)\})\big) > 0$.

1. Introduction

It is well-known that each Sobolev mapping $f\colon (0,1)^n \to \mathbf{R}^m$ is absolutely continuous on $\mathcal{H}^{n-1}$ almost all lines parallel to coordinate axes (see e.g. [16, Theorem 2.1.4]). It follows that $\mathcal{H}^1$ null sets on these lines are mapped to sets of $\mathcal{H}^1$ measure zero, i.e. that f satisfies the one dimensional Lusin (N) condition there.

In models of Nonlinear Elasticity (see e.g. [1]) it is moreover natural to expect that the mapping $f\colon (0,1)^n \to \mathbf{R}^n$ is moreover a homeomorphism because of the interpenetration of the matter and the same injectivity assumption is needed in Geometric Function Theory (see [7, 8] and references given there). For these homeomorphisms it is crucial to know that sets of zero $\mathcal{H}^n$ measure are mapped to sets of zero $\mathcal{H}^n$ measure as this corresponds to the fact that no material is "created" during our deformation. It was shown that this n-dimensional Lusin (N) condition is true for homeomorphisms in $W^{1,n}((0,1)^n, \mathbf{R}^n)$ by Reshetnyak [15] (see also [11, 14] or [7, Theorem 4.10] for sharpness).

Let us note that k-dimensional Lusin (N) conditions are crucial ingredients for various change of variables formulas and coarea formula (see e.g. [6], [7, Section A.8] and [12]) which are extremely important tools in the area. Each Sobolev mapping is approximatively differentiable a.e. and thus the area or coarea formula holds up to a null set and thus the validity of the k-dimensional Lusin condition is in fact equivalent to the validity of the formula.

The validity of the $(n-1)$-dimensional Lusin (N) condition for homeomorphism in $W^{1,n-1}((0,1)^n, \mathbf{R}^n)$ on $\mathcal{H}^1$ almost every hyperplane was shown by Csörnyei, Hencl and Malý in [4] and it was the crucial new ingredient in their result. Knowing these three results for $k = 1, n-1, n$ one could expect that the k-dimensional Lusin (N) condition holds for $W^{1,k}$ homeomorphisms for $\mathcal{H}^{n-k}$ almost every k-dimensional subspace. Such a result would be useful e.g. in [5, Theorem 12] as it would imply the validity of the result also in the borderline case $p = m$ without extra assumptions. The negative result would show the necessity of the Hölder continuity in [13, Theorem 2].

Below we show that unfortunately such a result is not true.

https://doi.org/10.5186/aasfm.2017.4244
2010 Mathematics Subject Classification: Primary 46E35.
Key words: Lusin's condition, Sobolev mapping.
Authors were supported by the ERC CZ grant LL1203 of the Czech Ministry of Education.

Theorem 1.1. *There exists a homeomorphism $F \in W^{1,2}((0,1)^4, \mathbf{R}^4)$ which fails the 2-dimensional Lusin's condition on $\mathcal{H}^2$ positively many hyperplanes. That is, there exists $\mathcal{C}_1 \subset [0,1]^2$ with $\mathcal{H}^2(\mathcal{C}_1) > 0$ such that for each $(z,w) \in \mathcal{C}_1$ there is a set $A_{(z,w)} \subset [0,1]^2$ with $\mathcal{H}^2(A_{(z,w)}) = 0$ and $\mathcal{H}^2\big(F(A_{(z,w)} \times \{(z,w)\})\big) > 0$.*

Let us note that in the above result we have even

$$\mathcal{H}^2\Big(\pi_{x,y}\big(F(A_{(x,y)} \times \{(z,w)\})\big)\Big) > 0$$

where $\pi_{x,y}(x,y,z,w) = (x,y)$ denotes the projection to the xy-plane. We expect that similarly it would be possible to construct a homeomorphism $f \in W^{1,k}((0,1)^n, \mathbf{R}^n)$ which fails k-dimensional Lusin's condition on $\mathcal{H}^{n-k}$ positively many k-dimensional subspaces for every $n \geq 4$ and $k \in \{2,3,\dots,n-2\}$. We have not pursued the details as the construction for $n=4$ and $k=2$ is already quite complicated.

Let us briefly explain the main idea of our construction. It is known by the Cesari's construction that there is a mapping $g \in W^{1,2}((0,1)^2, \mathbf{R}^2)$ which fails the two dimensional Lusin (N) condition (see [2] or [7, Theorem 4.3]) but unfortunately this mapping is far from being injective. We correct this by pushing the next steps of this construction to higher level in the third dimension and we construct a homeomorphism $\tilde{g}\colon (0,1)^2 \to \mathbf{R}^3$ which fails the 2-dimensional Lusin (N) condition. We use this construction for each $(z,w) \in \mathcal{C}_1$ and this is what our mapping F is essentially doing up to translation on the 2-dimensional subspace $(0,1)^2 \times \{(z,w)\}$. Around these points we do just some finite approximation of the construction so that the mapping is locally Lipschitz there and we do this cleverly so that the whole mapping is a homeomorphism. It is easy to control $\int_{\mathbf{R}^2 \times \{(z,w)\}} |DF|^2$ for $(z,w) \in \mathcal{C}_1$ as we know that $\tilde{g} \in W^{1,2}$. For most of the points $(z,w) \notin \mathcal{C}_1$ we know that F is Lipschitz on $\mathbf{R}^2 \times \{(z,w)\}$ but the Lipschitz constant may grow as we approach $\mathcal{C}_1$. However we can construct $\mathcal{C}_1$ so big that the $\mathcal{H}^2$-measure of those $(z,w) \notin \mathcal{C}_1$ is really small and this allows us to control $\int |DF|^2$ there.

1.1. Structure of the paper. Throughout the paper we will work in $\mathbf{R}^4$. The points in $\mathbf{R}^4$ are usually denoted as (x,y,z,w), and these letters are used primarily to distinguish the different coordinates i.e. w is the fourth coordinate. We use notation $\mathbf{x}$ and $\mathbf{y}$ for points in $\mathbf{R}^4$.

In Section 2.2 we define a Cantor set $\mathcal{C}_1$, with positive two dimensional measure. We will construct a mapping which fails Lusin's condition on every hyperplane $\mathbf{R}^2 \times \{(z,w)\}$, with $(z,w) \in \mathcal{C}_1$.

Our map is a composition of several homeomorphisms

$$F = u \circ \pi \circ S. \tag{1.1}$$

The mapping S is defined as $S(x,y,z,w) = (x,y,\tilde{S}(z,w))$, where $\tilde{S}$ is a frames-to-frames mapping squeezing Cantor set $\mathcal{C}_1$ onto $\mathcal{C}_2$ a Cantor set of small (but positive) Hausdorff dimension. Similarly, mapping π is defined $\pi(x,y,z,w) = (x,y,\tilde{\pi}(z,w))$, where $\tilde{\pi}\colon \mathbf{R}^2 \to \mathbf{R}^2$ is a bi-Lipschitz mapping which restricted on $\mathcal{C}_2$ is a projection on line $\{0\} \times \mathbf{R}$. The composition $\pi \circ S$ maps $\mathcal{C}_1$ to a certain Cantor set $\mathcal{C}_3$ on line $\{0\} \times \mathbf{R}$, while preserving planes parallel to $\{(0,0)\} \times \mathbf{R}^2$.

In Section 3 we construct a homeomorphism u, between 3-dimensional domains, which on the hyperplane $\mathbf{R}^2 \times \{0\}$ fails the 2-dimensional Lusin's condition. This is achieved with a construction similar to Cesari's construction [2].

Finally, we set $u(x,y,z,w) = (u(x,y,z),w)$ to obtain a homeomorphism which breaks the Lusin's condition on all hyperplanes $\mathbf{R}^2 \times \{(0,w)\}$ for $w \in \mathcal{C}_3$.

2. Preliminaries

2.1. Notation. By e_i we denote the basis vectors in $\mathbf{R}^4$, i.e. $e_1 = (1,0,0,0)$ and so on.

Throughout the paper $|Mat|$ is the matrix with elements $\{|Mat_{i,j}|\}_{i,j=1}^n$ and in context of matrices "$\lesseqqgtr$" and "$\leq$" should be understood elementwise. Notice that for all matrices A, B, C, D with positive entries we have that if $A \leq B$ and $C \leq D$ also

$$AC \leq BD$$

when the multiplications are defined.

For $f\colon (0,1)^n \to \mathbf{R}^n$ we use the notation $\partial_i f$ for the partial derivative with respect to i-th coordinate x_i and by Df we denote the matrix of all derivatives, i.e. the i-th column of Df is $\partial_i f$. We denote the usual m-dimensional Hausdorff measure by $\mathcal{H}^m$.

2.2. Construction of the squeezing map $\boldsymbol{S}$. In this subsection we define the first part of our homeomorphism. On two coordinates the mapping is a typical frames-to-frames mapping squeezing a Cantor set $\mathcal{C}_1$ of positive 2-dimensional measure to a Cantor set $\mathcal{C}_2$ of dimension strictly smaller than 2. On two remaining coordinates the mapping is the identity. The idea of the construction goes back to Ponomarev [14] (see also [9, Section 5] and [7, Chapter 4.3]).

We will first give two Cantor set constructions in $(0,1)^2$. Our mapping $\tilde{S}$ will be defined as a limit of a sequence of piecewise continuously differentiable homeomorphisms $S_k\colon (0,1)^2 \to (0,1)^2$, where each S_k maps the k-th step of the first Cantor set construction onto the second one. Then the limit mapping $\tilde{S}$ maps the first Cantor set onto the second one. This mapping could be extended by identity outside of $(0,1)^2$.

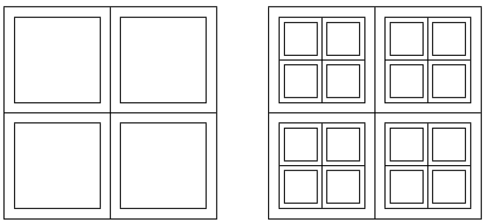

Figure 1. Cubes $Q_{\boldsymbol{v}}$ and $Q'_{\boldsymbol{v}}$ for $\boldsymbol{v} \in \mathbf{V}^1$ and $\boldsymbol{v} \in \mathbf{V}^2$.

By $\mathbf{V}$ we denote the set of 4 vertices of the cube $[-1,1]^2$. The sets $\mathbf{V}^k = \mathbf{V} \times \ldots \times \mathbf{V}$, $k \in \mathbf{N}$, will serve as the sets of indices for our construction. Let $\gamma > 0$ be a fixed constant whose value we specify later and let us denote

$$\varphi(k) = \frac{1}{2}(1 + 4^{-k}) \quad \text{and} \quad b_k = 2^{-\gamma k}. \tag{2.1}$$

Set $z_0 = \tilde{z}_0 = (\frac{1}{2}, \frac{1}{2})$ and let us define

$$r_k = \frac{1}{2}\varphi(k)2^{-k} \quad \text{and} \quad \tilde{r}_k = \frac{1}{2}b_k 2^{-k}. \tag{2.2}$$

It follows that $(0,1)^2 = Q(z_0, r_0) = Q(\tilde{z}_0, \tilde{r}_0)$ and further we proceed by induction. For $\boldsymbol{v} = [v_1, \ldots, v_k] \in \mathbf{V}^k$ we denote $\boldsymbol{w} = [v_1, \ldots, v_{k-1}]$ and we define (see Figure 1)

$$z_{\boldsymbol{v}} = z_{\boldsymbol{w}} + \frac{1}{2}r_{k-1}v_k = z_0 + \frac{1}{2}\sum_{j=1}^{k} r_{j-1}v_j, \quad Q'_{\boldsymbol{v}} = Q(z_{\boldsymbol{v}}, \tfrac{r_{k-1}}{2}) \quad \text{and} \quad Q_{\boldsymbol{v}} = Q(z_{\boldsymbol{v}}, r_k).$$

Formally we should write $\boldsymbol{w}(\boldsymbol{v})$ instead of $\boldsymbol{w}$ but for the simplification of the notation we will avoid this.

The number of the cubes $\{Q_{\boldsymbol{v}} \colon \boldsymbol{v} \in \mathbf{V}^k\}$ is 4^k. It is not difficult to find out that the resulting Cantor set

$$\mathcal{C}_1 := \bigcap_{k=1}^{\infty} \bigcup_{\boldsymbol{v}\in\mathbf{V}^k} Q_{\boldsymbol{v}}$$

is a product of two Cantor sets in $\mathbf{R}$. Moreover, $\mathcal{H}^2(\mathcal{C}_1) > 0$ since

$$\mathcal{H}^2\Bigg(\bigcup_{\boldsymbol{v}\in\mathbf{V}^k} Q_{\boldsymbol{v}}\Bigg) = 4^k(\varphi(k)2^{-k})^2 \overset{k\to\infty}{\to} \frac{1}{4}.$$

Analogously we define

$$\tilde{z}_{\boldsymbol{v}} = \tilde{z}_{\boldsymbol{w}} + \frac{1}{2}\tilde{r}_{k-1}v_k = \tilde{z}_0 + \frac{1}{2}\sum_{j=1}^{k}\tilde{r}_{j-1}v_j, \quad \tilde{Q}'_{\boldsymbol{v}} = Q(\tilde{z}_{\boldsymbol{v}}, \tfrac{\tilde{r}_{k-1}}{2}) \quad \text{and} \quad \tilde{Q}_{\boldsymbol{v}} = Q(\tilde{z}_{\boldsymbol{v}}, \tilde{r}_k).$$

The resulting Cantor set

$$\mathcal{C}_B := \bigcap_{k=1}^{\infty} \bigcup_{\boldsymbol{v}\in\mathbf{V}^k} \tilde{Q}_{\boldsymbol{v}}$$

satisfies $\mathcal{H}^2(\mathcal{C}_B) = 0$ since $\lim_{k\to\infty} b_k = 0$. It remains to find a homeomorphism $\tilde{S}$ which maps $\mathcal{C}_1$ onto $\mathcal{C}_2$.

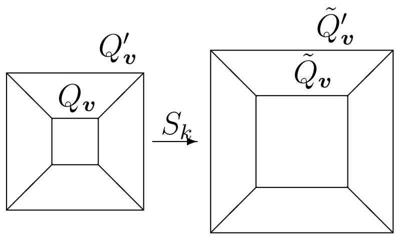

Figure 2. The transformation of $Q'_v \setminus Q^\circ_v$ onto $\tilde{Q}'_v \setminus \tilde{Q}^\circ_v$.

We will find a sequence of homeomorphisms $S_k \colon (0,1)^2 \to (0,1)^2$. We set $S_0(\mathbf{x}) = \mathbf{x}$ and we proceed by induction. We will give a mapping S_1 which stretches each cube Q_v, $v \in \mathbf{V}^1$, homogeneously so that $S_1(Q_v)$ equals $\tilde{Q}_v$. On the annulus $Q'_v \setminus Q_v$, S_1 is defined to be an appropriate radial map with respect to z_v and $\tilde{z}_v$ in the image in order to make S_1 a homeomorphism. The general step is the following: If $k > 1$, S_k is defined as S_{k-1} outside the union of all cubes $Q_{\boldsymbol{w}}$, $\boldsymbol{w} \in \mathbf{V}^{k-1}$. Further, S_k remains equal to S_{k-1} at the centers of cubes $Q_{\boldsymbol{v}}$, $\boldsymbol{v} \in \mathbf{V}^k$. Then S_k stretches each cube $Q_{\boldsymbol{v}}$, $\boldsymbol{v} \in \mathbf{V}^k$, homogeneously so that $S_k(Q_{\boldsymbol{v}})$ equals $\tilde{Q}_{\boldsymbol{v}}$. On the annulus $Q'_{\boldsymbol{v}} \setminus Q_{\boldsymbol{v}}$, S_k is defined to be an appropriate radial map with respect to $z_{\boldsymbol{v}}$ in preimage and $\tilde{z}_{\boldsymbol{v}}$ in image to make S_k a homeomorphism (see Figure 2). Notice that the Jacobian determinant $J_{S_k}(\mathbf{x})$ will be strictly positive almost everywhere in $(0,1)^n$.

In this construction we use the notation $\|\mathbf{x}\|$ for the supremum norm of $\mathbf{x} \in \mathbf{R}^2$. The mappings S_k, $k \in \mathbf{N}$, are formally defined as

$$(2.3) \quad S_k(\mathbf{x}) = \begin{cases} S_{k-1}(\mathbf{x}) & \text{for } \mathbf{x} \notin \bigcup_{\boldsymbol{v}\in\mathbf{V}^k} Q'_{\boldsymbol{v}}, \\ S_{k-1}(z_{\boldsymbol{v}}) + (\alpha_k\|\mathbf{x} - z_{\boldsymbol{v}}\| + \beta_k)\frac{x - z_{\boldsymbol{v}}}{\|x - z_{\boldsymbol{v}}\|} & \text{for } \mathbf{x} \in Q'_{\boldsymbol{v}} \setminus Q_{\boldsymbol{v}},\ \boldsymbol{v} \in \mathbf{V}^k, \\ S_{k-1}(z_{\boldsymbol{v}}) + \frac{\tilde{r}_k}{r_k}(\mathbf{x} - z_{\boldsymbol{v}}) & \text{for } \mathbf{x} \in Q_{\boldsymbol{v}},\ \boldsymbol{v} \in \mathbf{V}^k, \end{cases}$$

where the constants α_k and β_k are given by

$$\alpha_k r_k + \beta_k = \tilde{r}_k \quad \text{and} \quad \alpha_k \frac{r_{k-1}}{2} + \beta_k = \frac{\tilde{r}_{k-1}}{2}. \tag{2.4}$$

It is not difficult to find out that each S_k is a homeomorphism and maps

$$\bigcup_{\boldsymbol{v}\in\mathbf{V}^k} Q_{\boldsymbol{v}} \quad \text{onto} \quad \bigcup_{\boldsymbol{v}\in\mathbf{V}^k} \tilde{Q}_{\boldsymbol{v}}.$$

The limit $\tilde{S}(\mathbf{x}) = \lim_{k\to\infty} S_k(\mathbf{x})$ is clearly one to one and continuous and therefore a homeomorphism. Moreover, it is not difficult to see that S is differentiable almost everywhere, absolutely continuous on almost all lines parallel to coordinate axes and maps $\mathcal{C}_1$ onto $\mathcal{C}_2$ (see [7, Chapter 4.3] for details).

Let $k \in \mathbf{N}$ and $\boldsymbol{v} \in \mathbf{V}^k$. We need to estimate $D\tilde{S}(\mathbf{x})$ in the interior of the annulus $Q'_{\boldsymbol{v}} \setminus Q_{\boldsymbol{v}}$. Since

$$\tilde{S}(\mathbf{x}) = \tilde{S}(z_{\boldsymbol{v}}) + (\alpha_k\|\mathbf{x} - z_{\boldsymbol{v}}\| + \beta_k)\frac{x - z_{\boldsymbol{v}}}{\|x - z_{\boldsymbol{v}}\|}$$

we obtain analogously to [7, Chapter 4.3] that

$$|D\tilde{S}(\mathbf{x})| \sim \max\left\{\frac{\tilde{r}_k}{r_k}, \alpha_k\right\} = \max\left\{\frac{b_k}{\varphi(k)}, \frac{b_{k-1} - b_k}{\varphi(k-1) - \varphi(k)}\right\} \sim 2^{2k-\gamma k}. \tag{2.5}$$

and

$$J_{\tilde{S}^{-1}}(\mathbf{x}) \lesssim (\varphi(k-1) - \varphi(k))2^{2\gamma k} \lesssim 2^{2(\gamma-1)k}. \tag{2.6}$$

Our squeezing map $S\colon \mathbf{R}^4 \to \mathbf{R}^4$ is defined as

$$S(x_1, x_2.x_3, x_4) = (x_1, x_2, \tilde{S}_1(x_3, x_4), \tilde{S}_2(x_3, x_4)).$$

If x is a point such that $(x_3, x_4) \in \mathcal{C}_1$, then we have

$$D\tilde{S}(x_3, x_4) = 0.$$

Actually, on this set the function is differentiable in the classical sense as can be seen from the definition. Therefore

$$|DS(\mathbf{x})| = 1 \text{ and } J_S(\mathbf{x}) = 0 \tag{2.7}$$

there.

2.3. Construction of the projection mapping $\boldsymbol{\pi}$. We define

$$\pi(x, y, z, w) = (x, y, \tilde{\pi}(z, w))$$

where $\tilde{\pi}\colon \mathbf{R}^2 \to \mathbf{R}^2$ is a Lipschitz homeomorphism such that

$$\tilde{\pi}(\mathcal{C}_2) \subset \big\{(z, w)\colon z = 0\big\} \tag{2.8}$$

which we construct below. By properties of bi-Lipschitz maps we have for almost every $\mathbf{x} \in \mathbf{R}^4$

$$\frac{1}{L} \le D\pi(\mathbf{x}) \le L, \quad \frac{1}{L^2} \le J_\pi(\mathbf{x}) \le L^2, \tag{2.9}$$

where L is the Lipschitz constant of $\tilde{\pi}$. Let us note that the construction of $\tilde{\pi}$ is inspired by the similar construction in [3].

Let us denote by

$$Pr(z, w) = \Big(0, w + \frac{1}{2}z\Big)$$

the projection of $\mathbf{R}^2$ onto $\{(z, w)\colon z = 0\}$ in the direction of the vector $(-2, 1)$. To construct $\tilde{\pi}$ we choose γ big enough in the construction of $\mathcal{C}_2$ (see (2.1)). Then we obtain that the projection of cubes $Pr(Q_{\boldsymbol{v}})$, $\boldsymbol{v} \in \mathbf{V}^1$, are pairwise disjoint (see Figure 3).

As the construction of $\mathcal{C}_2$ is self-similar we obtain that the projection of cubes $Q_{\boldsymbol{v}}$, $\boldsymbol{v} \in \mathbf{V}^k$, are also pairwise disjoint. Therefore it is not difficult to see that the projection $Pr\colon C_2 \to \big\{(z,w)\colon z=0\big\}$ is in fact injective, i.e.

$$a, b \in \mathcal{C}_2,\ a \neq b \Rightarrow Pr(a) \neq Pr(b).$$

It follows that we can find a mapping $g\colon Pr(\mathcal{C}_2) \to \mathbf{R}$ such that the projection on $\mathcal{C}_2$ is given by

$$Pr(z,w) = (z,w) + g(Pr(z,w)) \cdot (-2,1) \ \text{ for every } (z,w) \in \mathcal{C}_2.$$

It is not difficult to see that g is a Lipschitz function and its Lipschitz constant can be estimated by

$$\frac{C}{\min\Big(\operatorname{dist}(Pr(Q_{\boldsymbol{v}}), Pr(Q_{\tilde{\boldsymbol{v}}}))\colon \boldsymbol{v},\ \tilde{\boldsymbol{v}} \in \mathbf{V}^1, \boldsymbol{v} \neq \tilde{\boldsymbol{v}}\Big)}.$$

It follows that we can extend this Lipschitz function g to a Lipschitz function $g\colon \mathbf{R} \to \mathbf{R}$. Now we can define

$$\tilde{\pi}(z,w) = (z,w) + g(Pr(z,w)) \cdot (-2,1) \ \text{ for every } (z,w) \in \mathbf{R}^2.$$

It is easy to see that $\tilde{\pi}$ is a Lipschitz homeomorphisms and moreover, that (2.8) holds. Moreover, the inverse of this mapping is given by

$$\tilde{\pi}^{-1}(z,w) = (z,w) - g(\tilde{\pi}(z,w)) \cdot (-2,1)$$

and hence $\tilde{\pi}$ is even bi-Lipschitz homeomorphism.

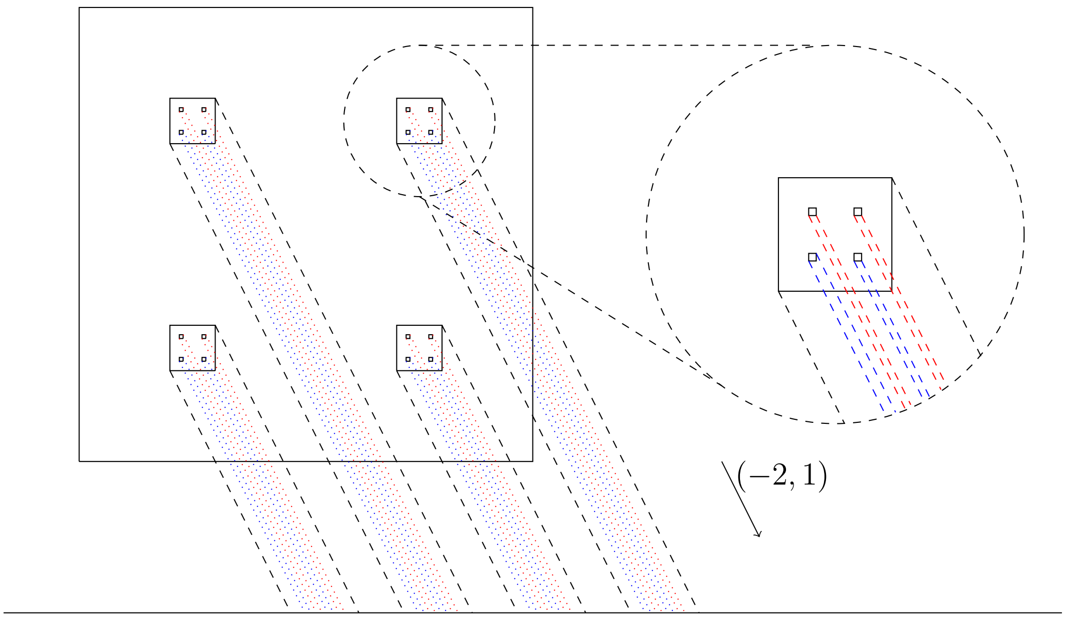

Figure 3. Projection is one to one—idea behind the self similarity argument.

2.4. Basic building block of $\boldsymbol{u}$. Assume that we are given eight points $a_1, a_2, a_3, a_4, b_1, b_2, b_3, b_4 \in \mathbf{R}^3$ such that points a_1, a_2, a_3, a_4 and b_1, b_2, b_3, b_4 are both a vertices of some non-degenerate convex quadrilaterals. We define a mapping $P := P_{a_i,b_i}\colon [0,1]^3 \to \mathbf{R}^3$ as

$$\begin{aligned} P(s,t,u) = a_1 &+ t(a_2 - a_1) + u(a_4 - a_1 + t(a_3 - a_4 + a_1 - a_2)) + s[b_1 - a_1 \\ &+ t(b_2 - a_2 + a_1 - b_1) + u(b_4 - a_4 - b_1 + a_1 \\ &+ t(b_3 - b_4 + b_1 - b_2 - a_3 + a_4 - a_1 + a_2))]. \end{aligned} \tag{2.10}$$

We now explain how to obtain the mapping above. First we parametrize quadrilateral a_1, a_2, a_3, a_4 with $\{0\} \times [0,1]^2$ and quadrilateral b_1, b_2, b_3, b_4 with $\{1\} \times [0,1]^2$ such that vertices are mapped to vertices. For a_1, a_2, a_3, a_4 we use the parametrization

$$P(0,t,u) = a_1 + t(a_2 - a_1) + u(a_4 - a_1 + t(a_3 - a_4 + a_1 - a_2)).$$

For the points b_i the mapping is defined similarly.

For other values of s we use linear interpolation (see Figure 4)

$$P(s,t,u) = (1-s)P(0,t,u) + sP(1,t,u).$$

We define

$$P(a_i, b_i) := P(a_1, a_2, a_3, a_4, b_1, b_2, b_3, b_4) = P([0,1]^3). \tag{2.11}$$

The second notation is justified by the fact that the set above is defined by the ordered set of vertices.

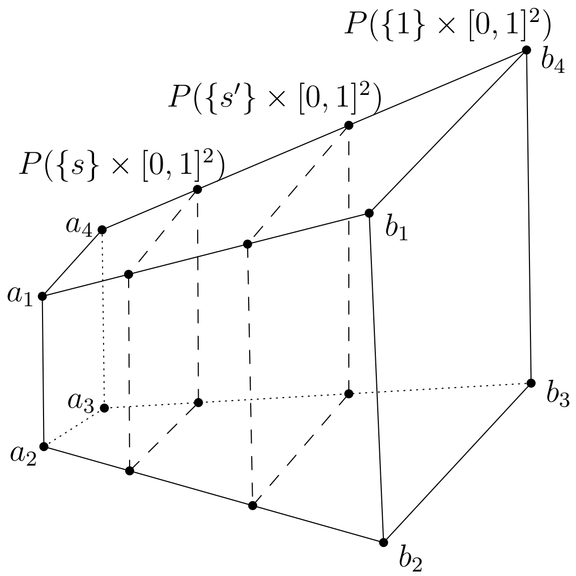

Figure 4. Image of $P([0,1]^3)$.

Remark 1. (1) Notice that the set $P(a_i, b_i)$ is not necessarily a polyhedron.

(2) Assume we are given two sets of eight points, K and L, and the corresponding mappings P_K and P_L, respectively. Then if on some face of $[0,1]^3$ the two mappings agree on vertices, then they agree on that face. This will be used later to show the continuity of mappings constructed from these mapping elements.

Conditions for homeomorphicity. Our main purpose is to construct a homeomorphism. The mapping P defined in (2.10) not a homeomorphism in general and we need some extra condition to guarantee this. The Lemma 2.2 is sufficient for us. The proofs are elementary and we provide only the outline of the proof.

Lemma 2.1. *Let $a, b, c, d \in \mathbf{R}^2$ be distinct points such that $Q = abcd$ is a convex non-degenerate quadrilateral. Then $P\colon [0,1]^2 \to Q$*

$$P(t,u) = a + t(b-a) + u[d - a + t(c - d + a - b)] \tag{2.12}$$

is a homeomorphism.

Proof. P is obviously continuous. We will prove it is also injection. For any given t the set $P(t,[0,1])$ is a line segment with endpoints $q_1(t) = a + t(b-a)$ and $q_2(t) = d + t(c-d)$. Moreover, it is easy to see (see Figure 5) that for $0 < t < t' < 1$ the line segments $P(t,[0,1])$ and $P(t',[0,1])$, with $t, t' \in (0,1)$ do not intersect. It follows that P is a homeomorphism. ☐

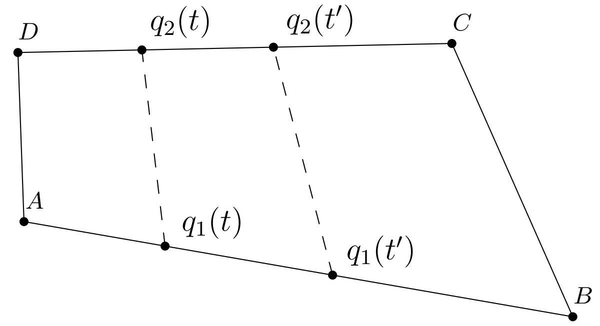

Figure 5. $P\colon [0,1]^2 \to Q$ is a homeomorphism.

Lemma 2.2. *If*

(1) *segments a_1a_2, a_3a_4, b_1b_2 and b_3b_4 are parallel,*
(2) *quadrilaterals $a_1a_2b_2b_1$ and $a_3a_4b_4b_3$ are disjoint,*
(3) *segments a_1b_1, a_2b_2, a_3b_3 and a_4b_4 are mutually disjoint and*
(4) *for $0 < s < s' < 1$ the sets $P(\{s\} \times [0,1]^2)$ and $P(\{s'\} \times [0,1]^2)$ are disjoint. (See Figure 4.)*

then P is a homeomorphism onto its image.

Proof. It is enough to show that P is injective. The condition (3) implies that all point $q_i(s) = (1-s)a_i + sb_i$ are all different. The condition (1) implies that line segments $q_1(s)q_2(s)$ and $q_3(s)q_4(s)$ are parallel, which again implies that $q_1q_2q_3q_4$ is a planar quadrilateral. Assumption (2) tells us that $q_1q_2q_3q_4$ is non-degenerate. This quadrilateral is convex because both $a_1a_2a_3a_4$ and $b_1b_2b_3b_4$ are.

Notice that Lemma 2.1 shows that $P|_{\{s\}\times[0,1]^2}$ is homeomorphism. By (4) we know that $P(\{s\} \times [0,1]^2)$ and $P(\{s'\} \times [0,1]^2)$ are disjoint for $s \neq s'$. Hence it is not difficult to see that P is indeed a homeomorphism. ☐

On the derivative of P. We will also need some information on the derivative of mapping P. We always have the trivial estimate (set $a_5 = a_1$ and $b_5 = b_1$)

$$|\partial_i P(s,t,u)| \lesssim \max\{|a_j - a_{j+1}|, |b_j - b_{j+1}|, |a_j - b_j| \colon j = 1,2,3,4\}. \tag{2.13}$$

In some cases we need better estimates and for this reason we record the formulas for derivatives for future reference. These are (see (2.10))

$$\begin{aligned} \partial_1 P(s,t,u) = {} & (b_1 - a_1)(1 - t - u) + t(b_2 - a_2) \\ & + u(b_4 - a_4 + t(b_1 - a_1 + a_2 - b_2 + b_3 - a_3 + a_4 - b_4)), \end{aligned} \tag{2.14}$$

$$\begin{aligned} \partial_2 P(s,t,u) = {} & (a_2 - a_1)(1 - s) + (b_2 - b_1)s \\ & + u[(1-s)(a_3 - a_4 + a_1 - a_2) + s(b_3 - b_4 + b_1 - b_2)] \end{aligned} \tag{2.15}$$

and

$$\partial_3 P(s,t,u) = (1-s)[(1-t)(a_4-a_1)+t(a_3-a_2)] + s[(1-t)(b_4-b_1)+t(b_3-b_2)]. \tag{2.16}$$

3. Construction of Cesari type mapping u

In this section we define homeomorphism between two hollow polyhedra (see Figures 6 and 7). The idea is to construct the homeomorphism by first decomposing both polyhedra into ten pieces and the mapping is first defined on those pieces using mappings defined in Subsection 2.4. These sets and the homeomorphism between them are later used in iteration process leading to the final homeomorphism.

In the next two subsections we will define these polyhedra, their decompositions and homeomorphisms from the pieces to $[0,1]^3$. After that we combine these mappings to obtain a homeomorphism from one polyhedron to another.

3.1. Domain polyhedra. Let $0<h<H$, $0<er<R$ and $R-r<H-h$. In the following list we have vertices of polyhedron

$$A := A(R,r,H,h) = \left(\left[-\frac{R}{2},\frac{R}{2}\right]^2 \times \left[-\frac{H}{2},\frac{H}{2}\right]\right) \setminus \left(\left[-\frac{r}{2},\frac{r}{2}\right]^2 \times \left[-\frac{h}{2},\frac{h}{2}\right]\right).$$

(1) $a_1 = \frac{R}{2}(e_1+e_2)+\frac{H}{2}e_3$	(13) $a_1' = \frac{r}{2}(e_1+e_2)+\frac{h}{2}e_3$
(2) $a_2 = \frac{R}{2}(-e_1+e_2)+\frac{H}{2}e_3$	(14) $a_2' = \frac{r}{2}(-e_1+e_2)+\frac{h}{2}e_3$
(3) $a_3 = \frac{R}{2}(-e_1-e_2)+\frac{H}{2}e_3$	(15) $a_3' = \frac{r}{2}(-e_1-e_2)+\frac{h}{2}e_3$
(4) $a_4 = \frac{R}{2}(e_1-e_2)+\frac{H}{2}e_3$	(16) $a_4' = \frac{r}{2}(e_1-e_2)+\frac{h}{2}e_3$
(5) $b_1 = \frac{R}{2}(e_1+e_2)$	(17) $b_1' = \frac{r}{2}(e_1+e_2)$
(6) $b_2 = \frac{R}{2}(-e_1+e_2)$	(18) $b_2' = \frac{r}{2}(-e_1+e_2)$
(7) $b_3 = \frac{R}{2}(-e_1-e_2)$	(19) $b_3' = \frac{r}{2}(-e_1-e_2)$
(8) $b_4 = \frac{R}{2}(e_1-e_2)$	(20) $b_4' = \frac{r}{2}(e_1-e_2)$
(9) $c_1 = \frac{R}{2}(e_1+e_2)-\frac{H}{2}e_3$	(21) $c_1' = \frac{r}{2}(e_1+e_2)-\frac{h}{2}e_3$
(10) $c_2 = \frac{R}{2}(-e_1+e_2)-\frac{H}{2}e_3$	(22) $c_2' = \frac{r}{2}(-e_1+e_2)-\frac{h}{2}e_3$
(11) $c_3 = \frac{R}{2}(-e_1-e_2)-\frac{H}{2}e_3$	(23) $c_3' = \frac{r}{2}(-e_1-e_2)-\frac{h}{2}e_3$
(12) $c_4 = \frac{R}{2}(e_1-e_2)-\frac{H}{2}e_3$	(24) $c_4' = \frac{r}{2}(e_1-e_2)-\frac{h}{2}e_3$.

This polyhedron is split into ten pieces: first to $A_- = A\cap\{z<0\}$ and $A_+ = A\cap\{z\geq 0\}$ and then both these pieces are split to five disjoint pieces. These pieces (in case of A_+) are the top A_{+t} and four quadrants $A_{+1}, A_{+2}, A_{+3}, A_{+4}$. They are defined as (see (2.11) for the definition of P)

$$\begin{aligned}
A_{+t} &= P(a_1', a_2', a_3', a_4', a_1, a_2, a_3, a_4),\\
A_{+1} &= P(b_1', b_2', a_2', a_1', b_1, b_2, a_2, a_1),\\
A_{+2} &= P(b_2', b_3', a_3', a_2', b_2, b_3, a_3, a_2),\\
A_{+3} &= P(b_3', b_4', a_4', a_3', b_3, b_4, a_4, a_3),\\
A_{+4} &= P(b_4', b_1', a_1', a_4', b_4, b_1, a_1, a_4).
\end{aligned} \tag{3.1}$$

Replacing a by c here we obtain the analogous decomposition for A_-.

Now we define mappings from these sets onto $[0,1]^3$. Since A_{+i}, $i=1,2,3,4$, are the same sets up to a rotation we describe this map for A_{+t} and A_{+4} only. Let us first consider the set A_{+4}. We define $f_{+4}\colon A_{+4}\to[0,1]^3$ by

$$f_{+4}(x,y,z)=\left(\frac{\log\frac{x}{r/2}}{\log\frac{R}{r}},\frac{y+x}{2x},\frac{z}{\frac{h}{2}+\frac{H-h}{2}\frac{2x-r}{R-r}}\right). \tag{3.2}$$

This mapping is essentially the inverse of mapping P defined in Section 2.4 precomposed with logarithmic scaling in one direction. For $i=1,2,3$ f_{+i} is defined as a $f_{+4}\circ R_i$ where R_i is the rotation mapping A_{+i} to A_{+4}.

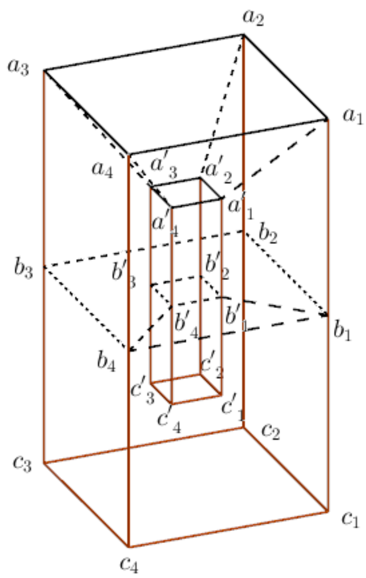

Figure 6. A picture of polyhedron A. We have marked with dashed lines the plane $z=0$ and the edges of A_{+t} and A_{+4}.

For the set A_{+t} we use the homeomorphism $f_{+t}\colon A_{+t}\to[0,1]^3$,

$$\begin{aligned}&f_{+t}(x,y,z)\\&=\left(\frac{\log\left[\frac{(2z-h)(R-r)}{r(H-h)}+1\right]}{\log\frac{R}{r}},\frac{x}{\frac{R-r}{H-h}(2z-h)+r}+\frac{1}{2},\frac{y}{\frac{R-r}{H-h}(2z-h)+r}+\frac{1}{2}\right).\end{aligned} \tag{3.3}$$

Also this mapping is obtained as a inverse of mapping defined in Section 2.4 composed with scaling. The scaling is chosen so that the final mapping defined in (3.17) below is continuous on $A_{+i}\cap A_{+t}$, for $i=1,2,3,4$. Finally we set $f_{-t}(x,y,z)=f_{+t}(x,y,-z)$.

Remark 2. (1) It is easy to check that all $f_{\pm i}$ are homeomorphisms. Moreover, they are Lipschitz with constants depending on H, h R, and r only.

(2) Notice, that all mappings $f_{\pm i}$ map points a_i, b_i, c_i onto corners of $\{1\}\times[0,1]^2$ and points a'_i, b'_i, c'_i onto corners of $\{0\}\times[0,1]^2$. Another thing to notice is that if the intersection $A_{\pm i}\cap A_{\pm j}$ is nonempty then the mappings $f_{\pm i}$ and $f_{\pm j}$ agree on this intersection.

Derivatives of $f_{\pm i}$. We also record the derivatives of these mappings for future reference

$$|Df_{+4}|(x,y,z)$$

$$(3.4)\qquad = \begin{vmatrix} \frac{1}{x}\left(\log\frac{R}{r}\right)^{-1} & 0 & 0 \\ -\frac{y}{2x^2} & \frac{1}{2x} & 0 \\ \frac{z\cdot\frac{H-h}{R-r}}{\left(\frac{h}{2}+\frac{H-h}{2}\frac{2x-r}{R-r}\right)^2} & 0 & \frac{1}{\frac{h}{2}+\frac{H-h}{2}\frac{2x-r}{R-r}} \end{vmatrix} \leq \begin{bmatrix} \frac{1}{x}\left(\log\frac{R}{r}\right)^{-1} & 0 & 0 \\ \frac{1}{x} & \frac{1}{2x} & 0 \\ \frac{z\cdot\frac{H-h}{R-r}}{\left(\frac{h}{2}+\frac{H-h}{2}\frac{2x-r}{R-r}\right)^2} & 0 & \frac{1}{\frac{h}{2}+\frac{H-h}{2}\frac{2x-r}{R-r}} \end{bmatrix},$$

$$(3.5)\qquad Df_{+t}(x,y,z) = \begin{bmatrix} 0 & 0 & \left(\log\frac{R}{r}\right)^{-1}\frac{2(R-r)}{(2z-h)(R-r)+r(H-h)} \\ \frac{1}{\frac{R-r}{H-h}(2z-h)+r} & 0 & \frac{-2x}{\left(\frac{R-r}{H-h}(2z-h)+r\right)^2}\frac{R-r}{H-h} \\ 0 & \frac{1}{\frac{R-r}{H-h}(2z-h)+r} & \frac{-2y}{\left(\frac{R-r}{H-h}(2z-h)+r\right)^2}\frac{R-r}{H-h} \end{bmatrix}.$$

It follows from (3.3) that

$$|x| \lessapprox \frac{R-r}{H-h}(2z-h)+r \quad\text{and}\quad |y| \lessapprox \frac{R-r}{H-h}(2z-h)+r.$$

With this and (3.5) we obtain the estimate

$$\|Df_{+t}(x,y,z)\| \lessapprox \frac{1}{\frac{R-r}{H-h}(2z-h)+r}\cdot\max\left\{1, \frac{R-r}{H-h}, \frac{R-r}{H-h}\left(\log\frac{R}{r}\right)^{-1}\right\}.$$

Eventually, we will choose these parameters so that $H-h > R-r$ and $\frac{R}{r} > e$ and in this case we have

$$(3.6)\qquad \|Df_{+t}(x,y,z)\| \lessapprox \frac{1}{\frac{R-r}{H-h}(2z-h)+r}.$$

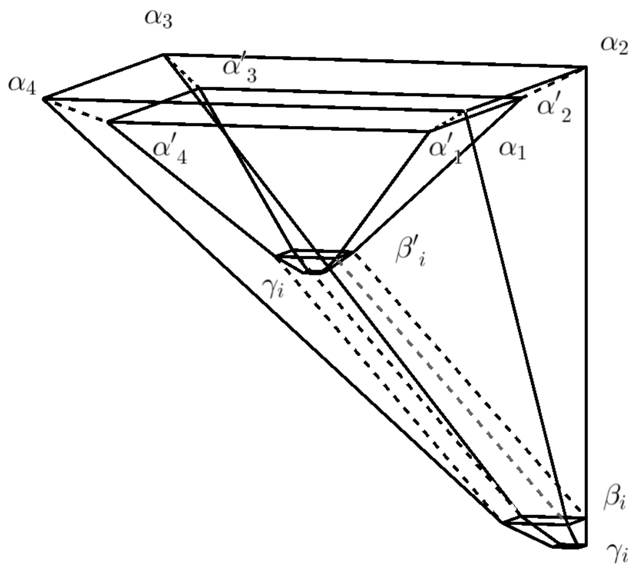

Figure 7. Polyhedron $T(j)$ it consists of polyhedron $S(j)$ with vertices α_i, β_i and γ_i minus polyhedron $U(j)$ with vertices α'_i, β'_i and γ'_i. We did not draw all points, but the points β_i et cetera are in similar order as points α_i.

3.2. Target polyhedra. Our aim is to construct a homeomorphism from A to the set $T(j)$, a polyhedron with a cavity, which is defined below (also see Figure 7).

To define the set we introduce several parameters. Let j be a positive integer. The used parameters are

$$(3.7)\qquad \varphi(j)=\frac{1}{2}(1+4^{-j}),\quad K_j=2^{-j-2}\varphi(j),\quad P_j=10^{-j}\quad\text{and}\quad T_j=1-10^{-j}.$$

We set

$$T(j)=S(j)\setminus U(j),$$

(see Figure 7) where $S(j)$ is the polyhedron with vertices

(1) $\alpha_1=2K_je_1+4^{-j}e_3$
(2) $\alpha_2=4^{-j}e_3$
(3) $\alpha_3=-2K_je_2+4^{-j}e_3$
(4) $\alpha_4=2K_j(e_1-e_2)+4^{-j}e_3$
(5) $\beta_1=\frac{P_j}{2}e_1$
(6) $\beta_2=0$
(7) $\beta_3=-\frac{P_j}{2}e_2$
(8) $\beta_4=\frac{P_j}{2}(e_1-e_2)$
(9) $\gamma_1=\frac{P_{j+1}^2}{2}e_1-\frac{P_{j+1}^3}{2}e_3$
(10) $\gamma_2=-\frac{P_{j+1}^3}{2}e_3$
(11) $\gamma_3=-\frac{P_{j+1}^2}{2}e_2-\frac{P_{j+1}^3}{2}e_3$
(12) $\gamma_4=\frac{P_{j+1}^2}{2}(e_1-e_2)-\frac{P_{j+1}^3}{2}e_3$

and $U(j)$, is the polyhedron with vertices

(1) $\alpha_1'=K_j(e_1-e_2)+2K_{j+1}(e_1+e_2)+4^{-j-1}(1+3T_j)e_3$
(2) $\alpha_2'=K_j(e_1-e_2)+2K_{j+1}(-e_1+e_2)+4^{-j-1}(1+3T_j)e_3$
(3) $\alpha_3'=K_j(e_1-e_2)+2K_{j+1}(-e_1-e_2)+4^{-j-1}(1+3T_j)e_3$
(4) $\alpha_4'=K_j(e_1-e_2)+2K_{j+1}(e_1-e_2)+4^{-j-1}(1+3T_j)e_3$
(5) $\beta_1'=K_j(e_1-e_2)+\frac{P_{j+1}}{2}(e_1+e_2)+3\cdot 4^{-j-1}T_je_3$
(6) $\beta_2'=K_j(e_1-e_2)+\frac{P_{j+1}}{2}(-e_1+e_2)+3\cdot 4^{-j-1}T_je_3$
(7) $\beta_3'=K_j(e_1-e_2)+\frac{P_{j+1}}{2}(-e_1-e_2)+3\cdot 4^{-j-1}T_je_3$
(8) $\beta_4'=K_j(e_1-e_2)+\frac{P_{j+1}}{2}(e_1-e_2)+3\cdot 4^{-j-1}T_je_3$
(9) $\gamma_1'=K_j(e_1-e_2)+\frac{P_{j+2}^2}{2}(e_1+e_2)+(3\cdot 4^{-j-1}T_j-\frac{P_{j+2}^3}{2})e_3$
(10) $\gamma_2'=K_j(e_1-e_2)+\frac{P_{j+2}^2}{2}(-e_1+e_2)+(3\cdot 4^{-j-1}T_j-\frac{P_{j+2}^3}{2})e_3$
(11) $\gamma_3'=K_j(e_1-e_2)+\frac{P_{j+2}^2}{2}(-e_1-e_2)+(3\cdot 4^{-j-1}T_j-\frac{P_{j+2}^3}{2})e_3$
(12) $\gamma_4'=K_j(e_1-e_2)+\frac{P_{j+2}^2}{2}(e_1-e_2)+(3\cdot 4^{-j-1}T_j-\frac{P_{j+2}^3}{2})e_3$.

Let us comment on the choice of these points. Notice that the center of square with vertices $\alpha_1,\alpha_2,\alpha_3$ and α_4 is

$$K_j(e_1-e_2)+4^{-j}e_3.$$

Similarly it is also a center of squares $\alpha_1'\alpha_2'\alpha_3'\alpha_4'$, $\beta_1'\beta_2'\beta_3'\beta_4'$ and $\gamma_1'\gamma_2'\gamma_3'\gamma_4'$ up to different third coordinate. Further, notice that by (3.7) we have

$$K_j>2K_{j+1},\quad K_j>\frac{P_{j+1}}{2}\quad\text{and}\quad K_j>\frac{P_{j+2}^2}{2}$$

which shows that the first term defining points α_i',β_i' and γ_i' is more important while the second is just a small adjustment. Finally the third term gives the proper height. Let us notice, that these expressions really give a set of points as displayed in Figure 7.

We split also the set $T(j)$ into ten pieces using the notation introduced in Section 2.4. These sets are

- $T_{+t} = P(\alpha_1', \alpha_2', \alpha_3', \alpha_4', \alpha_1, \alpha_2, \alpha_3, \alpha_4)$,
- $T_{+1} = P(\beta_1', \beta_2', \alpha_2', \alpha_1', \beta_1, \beta_2, \alpha_2, \alpha_1)$,
- $T_{+2} = P(\beta_2', \beta_3', \alpha_3', \alpha_2', \beta_2, \beta_3, \alpha_3, \alpha_2)$,
- $T_{+3} = P(\beta_3', \beta_4', \alpha_4', \alpha_3', \beta_3, \beta_4, \alpha_4, \alpha_3)$,
- $T_{+4} = P(\beta_4', \beta_1', \alpha_1', \alpha_4', \beta_4, \beta_1, \alpha_1, \alpha_4)$,
- $T_{-t} = P(\gamma_1', \gamma_2', \gamma_3', \gamma_4', \gamma_1, \gamma_2, \gamma_3, \gamma_4)$,
- $T_{-1} = P(\beta_1', \beta_2', \gamma_2', \gamma_1', \beta_1, \beta_2, \gamma_2, \gamma_1)$,
- $T_{-2} = P(\beta_2', \beta_3', \gamma_3', \gamma_2', \beta_2, \beta_3, \gamma_3, \gamma_2)$,
- $T_{-3} = P(\beta_3', \beta_4', \gamma_4', \gamma_3', \beta_3, \beta_4, \gamma_4, \gamma_3)$ and
- $T_{-4} = P(\beta_4', \beta_1', \gamma_1', \gamma_4', \beta_4, \beta_1, \gamma_1, \gamma_4)$.

In what follows we will use the mappings defined in Section 2.4 in order to map $[0,1]^3$ to $T_{\pm i}$ homeomorphically. This map is denoted by $g_{\pm i}\colon [0,1]^3 \to T_{\pm i}$, with $i = t, 1, 2, 3, 4$.

Homeomorphicity of $g_{\pm i}$. We use Lemma 2.2 to show that mappings $g_{\pm i}$ are homeomorphic. We will show some details for g_{+4}; the other mappings are similar. The conditions (1), (2) and (3) in these Lemmas are obvious from our choice of points. Now it is enough to show that $P(\{s\}\times[0,1]^2)$ does not intersect with $P(\{s'\}\times[0,1]^2)$ as in Figure 4. However, this is easy to see by our choice of points in T_{+4} (see Figure 7).

Derivatives of $g_{\pm i}$. In the end we will need estimates of derivatives of mappings $g_{\pm i}$, $i = t, 1, 2, 3, 4$. Notice that all points $\alpha_i, \beta_i, \gamma_i, \alpha_i', \beta_i'$ and γ_i' defined in the beginning of this section have norm bounded by $C2^{-j}$. With (2.13) this implies that

$$|Dg_{\pm i}| \lesssim 2^{-j} \quad \text{for } i \in \{1,2,3,4,t\}.$$

For $i \neq t$ we need finer estimates. We will explain only the case of g_{+4} and the set $T_{+4} = P(\beta_4', \beta_1', \alpha_1', \alpha_4', \beta_4, \beta_1, \alpha_1, \alpha_4)$. Other estimates are obtained similarly.

By (2.15) we have

$$\partial_2 g_{+4} = (\beta_1' - \beta_4')(1-s) + (\beta_1 - \beta_4)s + u[(1-s)(\alpha_1' - \alpha_4' + \beta_4' - \beta_1') + s(\alpha_1 - \alpha_4 + \beta_4 - \beta_1)].$$

Vectors $\beta_1 - \beta_4, \beta_1' - \beta_4'$, $\alpha_1 - \alpha_4$ and $\alpha_1' - \alpha_4'$ are all parallel to e_2. Moreover, $|\beta_1 - \beta_4| \leq P_j$ and the same applies to $|\beta_1' - \beta_4'|$. It follows that

$$|\partial_2 g_{+4}(s,t,u)| \lesssim P_j + 2^{-j} u$$

and that $\partial_2 g_{+4}(s,t,u)$ is parallel to e_2.

We collect the estimates for previous paragraphs into following matrix

$$|Dg_{\pm i}|(s,t,u) \lessapprox \begin{bmatrix} 2^{-j} & 0 & 2^{-j} \\ 2^{-j} & P_j + u2^{-j} & 2^{-j} \\ 2^{-j} & 0 & 2^{-j} \end{bmatrix} \tag{3.8}$$

with $i = 2, 4$ and

$$|Dg_{\pm i}|(s,t,u) \lessapprox \begin{bmatrix} P_j + u2^{-j} & 2^{-j} & 2^{-j} \\ 0 & 2^{-j} & 2^{-j} \\ 0 & 2^{-j} & 2^{-j} \end{bmatrix} \tag{3.9}$$

with $i = 1, 3$. Here $|Mat|$ is the matrix with elements $\{|Mat_{i,j}|\}_{i,j=1}^n$ and "$\lessapprox$" is understood elementwise.

Similarly we get using (2.14), (2.15) and (2.16) for $T_{+t} = P(\alpha'_1, \alpha'_2, \alpha'_3, \alpha'_4, \alpha_1, \alpha_2, \alpha_3, \alpha_4)$

$$|Dg_{\pm t}|(s,t,u) \lessapprox \begin{bmatrix} 2^{-j} & 2^{-j} & 0 \\ 2^{-j} & 0 & 2^{-j} \\ 2^{-j} & 0 & 0 \end{bmatrix} \tag{3.10}$$

and also

$$\|Dg_{\pm t}(s,t,u)\| \lessapprox 2^{-j}. \tag{3.11}$$

3.3. Compositions of $g_{\pm i}$ and $f_{\pm i}$. In this section we will define the main pieces in the construction of map u. We fix $\beta > 0$ large enough whose exact value will be fixed later. We set

$$R_j = \exp(-j^{\beta+1}) \tag{3.12}$$

and

$$r_j = 2R_{j+1}. \tag{3.13}$$

Using the mean value theorem we obtain for large j

$$\log \frac{R_j}{r_j} \approx \beta j^{\beta}. \tag{3.14}$$

Recall that γ was introduced in (2.1) and set

$$H_j = 2^{(-\gamma-1)j-1} \tag{3.15}$$

and

$$h_j = 2^{(-\gamma-1)(j+1)-1}. \tag{3.16}$$

It is easy to check that we have $0 < er_j < R_j$, $0 < h_j < H_j$ and for big values of j also $R_j - r_j < H_j - h_j$ as desired.

The map we are going to define in this section is a homeomorphism

$$u_j \colon A(R_j, r_j, H_j, h_j) \to T(j).$$

We do this by first defining maps from $A_{\pm i}$ to $T_{\pm i}$.

Composing homeomorphism $f_{\pm i}$ and $g_{\pm i}$ we obtain a homeomorphism

$$u_{\pm i} = g_{\pm i} \circ f_{\pm i} \colon A_{\pm i} \to T_{\pm i}.$$

These $u_{\pm i}$ map points a_i, b_i, c_i to points $\alpha_i, \beta_i, \gamma_i$, respectively, for every i for which map in question is defined.

We define the mapping

$$\tilde{u} \colon A \to T(j) \quad \text{as} \quad \tilde{u}|_{A_{\pm i}} = u_{\pm i}. \tag{3.17}$$

Notice, that these mappings agree on intersections of $A_{\pm i}$, where $i = 1, 2, 3, 4, t$, if they are not empty and mappings are defined on those intersections. This is quite easy to see. These intersections are faces of polyhedra $A_{\pm i}$ and we know that mappings agree on the vertices. Moreover, notice that the logarithmic scaling used in the definition of $f_{\pm i}$ affects only the first coordinate and with observations of Remark 2 it follows from our definitions of $g_{\pm i}$ and $f_{\pm i}$ that mappings agree on intersections. This gives a rise to a homeomorphism $\tilde{u} \colon A \to T(j)$ defined as $\tilde{u}|_{A_{\pm i}} = u_{\pm i}$.

Estimates of derivatives. Next we will show that certain estimates for derivatives hold on A_{+4} and A_{+t}.

Let us write

$$\rho(x,y,z) = \frac{\log\frac{x}{r_j/2}}{\log\frac{R_j}{r_j}} \quad \text{and} \quad \omega(x,y,z) = \frac{z}{\frac{h_j}{2} + \frac{H_j-h_j}{2}\frac{2x-r_j}{R_j-r_j}}.$$

These are the first and third component of f_{+4} respectively (see (3.2)). By (3.4) and (3.8) we have the following estimate for the partial derivatives

$$\begin{aligned}
|D\tilde{u}|(x,y,z) &= |Dg_{+4}(f_{+4}(x,y,z)) \cdot Df_{+4}(x,y,z)| \\
&\lessapprox \begin{bmatrix} 2^{-j} & 0 & 2^{-j} \\ 2^{-j} & P_j + \omega 2^{-j} & 2^{-j} \\ 2^{-j} & 0 & 2^{-j} \end{bmatrix} \cdot \begin{bmatrix} \frac{1}{x}\left(\log\frac{R}{r}\right)^{-1} & 0 & 0 \\ \frac{1}{x} & \frac{1}{2x} & 0 \\ \frac{\frac{H_j-h_j}{R_j-r_j}\omega}{\frac{h_j}{2}+\frac{H_j-h_j}{2}\frac{2x-r_j}{R_j-r_j}} & 0 & \frac{1}{\frac{h_j}{2}+\frac{H_j-h_j}{2}\frac{2x-r_j}{R_j-r_j}} \end{bmatrix} \\
&\lessapprox \begin{bmatrix} \frac{2^{-j}}{x}\left(\log\frac{R}{r}\right)^{-1} & 0 & 0 \\ \frac{2^{-j}}{x}\left(\log\frac{R}{r}\right)^{-1} + (P_j+\omega 2^{-j})\frac{1}{x} & \frac{P_j+\omega 2^{-j}}{2x} & 0 \\ \frac{2^{-j}}{x}\left(\log\frac{R}{r}\right)^{-1} & 0 & 0 \end{bmatrix} \\
&\quad + \frac{2^{-j}}{\frac{h_j}{2}+\frac{H_j-h_j}{2}\frac{2x-r_j}{R_j-r_j}} \begin{bmatrix} \frac{H_j-h_j}{R_j-r_j}\omega & 0 & 1 \\ \frac{H_j-h_j}{R_j-r_j}\omega & 0 & 1 \\ \frac{H_j-h_j}{R_j-r_j}\omega & 0 & 1 \end{bmatrix}.
\end{aligned} \tag{3.18}$$

To simplify these estimates we notice that

$$R_j - r_j \geq \frac{1}{2}x$$

for all large j. This gives (see (3.15) and (3.16))

$$\frac{2^{-j}}{\frac{h_j}{2}+\frac{H_j-h_j}{2}\frac{2x-r_j}{R_j-r_j}} \frac{H_j-h_j}{R_j-r_j} \lesssim \frac{2^{-j}}{H_j}\frac{H_j}{x} = \frac{2^{-j}}{x}. \tag{3.19}$$

Now from (3.18) and (3.19) we obtain that on A_{+4} for all large j we have

$$|D\tilde{u}|\,(x,y,z) \lesssim \frac{2^{-j}}{x}. \tag{3.20}$$

If $z=0$ we have $\omega = 0$ and together with the facts

$$2^{(c+1)j}R_j \leq \left(\log\frac{R_j}{r_j}\right)^{-1} \quad \text{and} \quad P_j \leq 2^{-j}\left(\log\frac{R_j}{r_j}\right)^{-1}$$

we obtain for $z=0$ slightly better estimate

$$|D\tilde{u}|\,(x,y,0) \lesssim \frac{2^{-j}}{x}\left(\log\frac{R}{r}\right)^{-1} \lesssim \frac{2^{-j}j^{-\beta}}{x}. \tag{3.21}$$

For the set A_{+t}, using (3.6) and (3.11), we get the estimate

$$\|D\tilde{u}(x,y,z)\| \lessapprox \frac{2^{-j}}{\frac{R_j-r_j}{H_j-h_j}(2z-h_j)+r_j}. \tag{3.22}$$

Blocks and flowers. Let the $Rot(\theta)$ be the rotation matrix of angle θ around z-axis. Later it is convenient for us to map several of the sets A (defined in Subsection 3.1) at the same time. To this end we define a block

$$Bl(R,r,H,h)=\bigcup_{i=0}^{4} Rot\Big(i\frac{\pi}{2}\Big)\Big(A+\frac{R}{2}(e_1-e_2)\Big) \tag{3.23}$$

and a flower (see Figure 8 and Figure 9)

$$Fl(j)=\bigcup_{i=0}^{4} Rot\Big(i\frac{\pi}{2}\Big)T(j). \tag{3.24}$$

Further we define a mapping

$$u_{Bl(R,r,H,h)}\colon Bl(R,r,H,h)\to Fl(j) \tag{3.25}$$

by

$$u|_{Rot^i(A+\frac{R}{2}(e_1-e_2))}(x)=Rot\Big(i\frac{\pi}{2}\Big)\tilde{u}\Big(Rot(-i\frac{\pi}{2})x\Big). \tag{3.26}$$

The set $[-R,R]^2\times[-\frac{H}{2},\frac{H}{2}]$ in Figure 8 is divided into four pieces and u is mapping each of these pieces onto corresponding big flowers. In the middle of each piece we have a block (see the shaded regions in Figure 8) that will be used in the next steps of the construction. We will divide this block again into four smaller pieces and map each piece onto smaller flower which lies inside the big flower. Below we describe in detail how we proceed further by induction and we define smaller and smaller pieces inside that are mapped to smaller and smaller flowers.

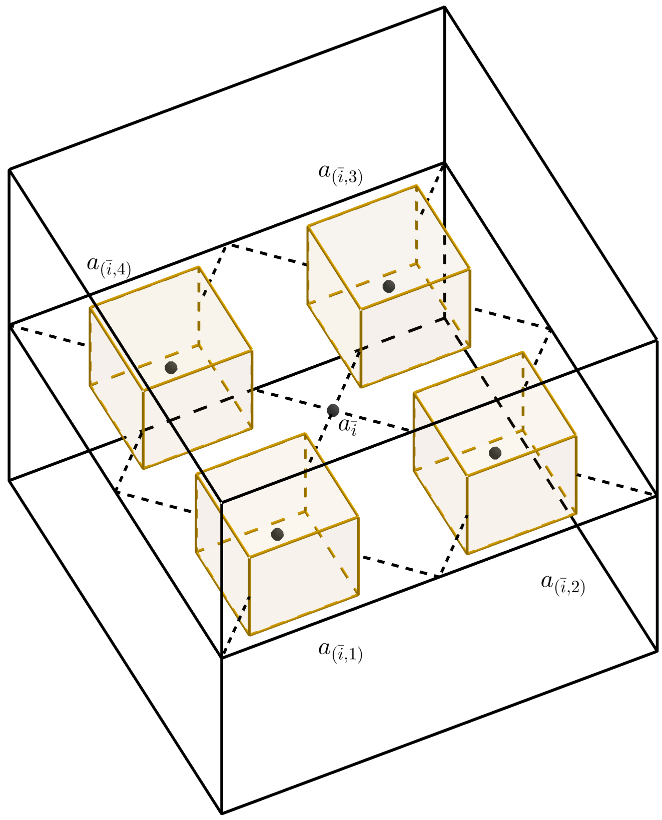

Figure 8. The set $Bl(R_j,r_j,H_j,h_j)$. The points marked in the picture are needed later.

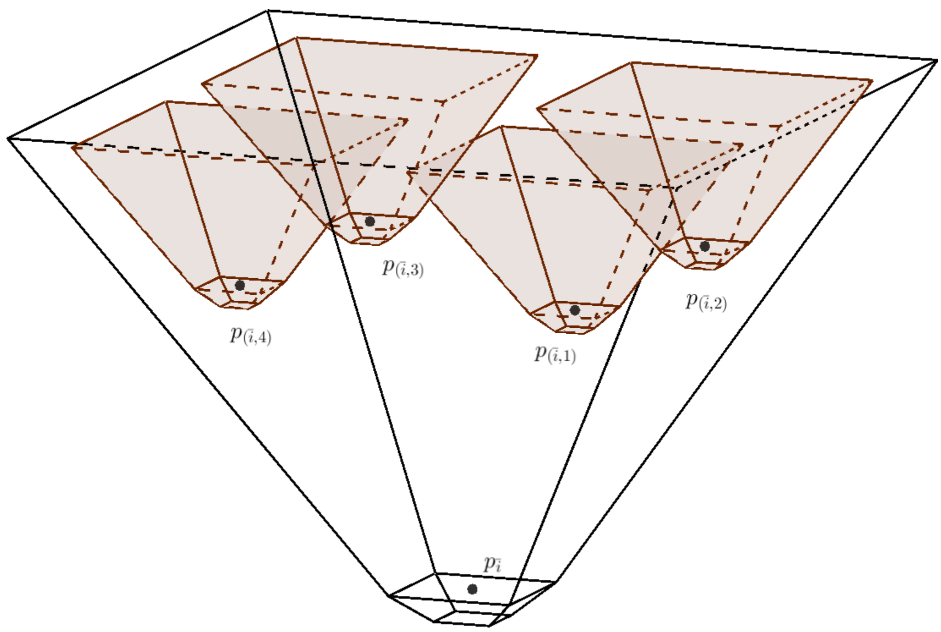

Figure 9. The set $Fl(j)$. The points marked in the picture are needed later.

Remark 3. Notice that by our construction $u_{Bl(R,r,H,h)}$ maps all faces of $Bl(R,r,H,h)$ onto faces of $Fl(j)$. Moreover, it is easy to see that the restrictions of $u_{Bl(R,r,H,h)}$ on any of these faces is essentially like the mappings defined in Subsection 2.4. Again we have the property that if we know the images of corners of the face the mapping is uniquely defined. We will use this in the next Subsection.

3.4. Construction of $\boldsymbol{u}$. We start by decomposing the three dimensional hyperplanes in the domain into blocks and in the codomain into flowers. Then, using the mapping defined in previous subsection, we obtain a homeomorphism between domains in $\mathbf{R}^3$. This map is then extended to a homeomorphism between domains in $\mathbf{R}^4$ by defining the map as identity in the fourth coordinate.

In order to describe the above mentioned decomposition to blocks and flowers describe a sequence of points used as centers of suitable blocks. To this end we recall the multi-index notation. Finite sequences $\bar{i} = (i_1, i_2, \dots, i_j)$, with $i_k \in \{1,2,3,4\}$ and $j \in \mathbf{N}$, are called multi-indices. The length of a multi-index is the number of its components and is denoted by $l(\bar{i})$. The set of all multi-indices is denoted by $\mathcal{I}$ and the set of all multi-indices of length j by $\mathcal{I}_j$.

Let $\omega\colon \{1,2,3,4\} \to \{e_1+e_2, e_1-e_2, -e_1+e_2, -e_1-e_2\}$ be some bijection. We define points (recall that R_k are defined in (3.12))

$$a_{\bar{i}} = a_{(i_1,i_2,\dots,i_j)} := \sum_{k=1}^{j} \frac{R_k}{2}\omega(i_k).$$

For locations of these points in construction see Figures 8 and 10.

In what follows we are interested in blocks

$$Bl\left(R_j, r_j, \frac{2^{-(\gamma+1)j}}{2}, \frac{2^{-(\gamma+1)(j+1)}}{2}\right) + a_{\bar{i}},$$

where $j \in \mathbf{N}$ and $\bar{i} \in \mathcal{I}_j$. From now on we will abuse the notation and write

$$Bl(j,\bar{i}) \quad \text{for} \quad Bl\left(R_j, r_j, \frac{2^{-(\gamma+1)j}}{2}, \frac{2^{-(\gamma+1)(j+1)}}{2}\right) + a_{\bar{i}}.$$

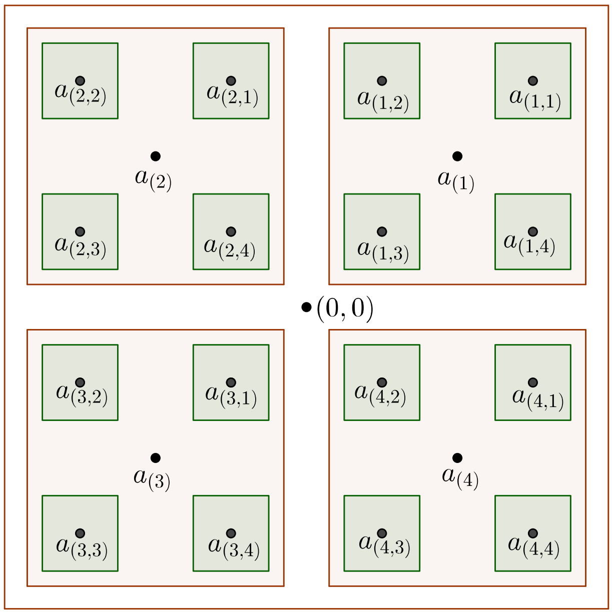

Figure 10. First generations of $Bl(R_j, r_j, H_j, h_j)$ with points $a_{\bar{i}}$ in the xy-plane.

Let us note that by (3.13), (3.15) and (3.16) the size of smaller blocks inside (the shaded parts in Figure 8) correspond to the size of the big blocks of the next generation.

The analogous pieces in the codomain are defined similarly. First, we define points (recall that T_k and K_k are defined in (3.7))

$$p_{\bar{i}} = \sum_{k=1}^{j} \left(K_k \omega(i_k) + 3 \cdot 4^{-k-1} T_k e_3 \right).$$

For locations of these points in construction see Figure 9. Again, we abuse the notation and denote

$$Fl(j, \bar{i}) := Fl(j) + p_{\bar{i}}.$$

Given the set $Fl(j, \bar{i})$ we notice that sets $Fl(j+1, (\bar{i}, i_{j+1}))$ intersect $Fl(j, \bar{i})$ only on the boundaries of its four cavities. Easiest way to see this is to check that vertices of certain $Fl(j+1, (\bar{i}, i_{j+1}))$ are exactly the vertices of one of the cavities. This is enough since both the cavities and the sets $Fl(j+1, (\bar{i}, i_{j+1}))$ are polyhedrons. By definition the vertices of $Fl(j+1)$ are obtained by rotating points α_4, β_4 and γ_4 around z-axis. These points are

$$\left\{ 2K_{j+1}(\pm e_1 \pm e_2) + 4^{-j-1} e_3,\ \frac{P_{j+1}}{2}(\pm e_1 \pm e_2),\ \frac{P^2_{j+2}}{2}(\pm e_1 \pm e_2) - \frac{P^3_{j+2}}{2} e_3 \right\}$$

On the other hand, the vertices of the cavity $U(j)$ of the set $T(j)$ defined in Subsection 3.2 are the points α'_i, β'_i and γ'_i. These differ from vertices of $Fl(j+1)$ by $K_j(e_1 - e_2) + 3 \cdot 4^{-j-1} T_j e_3$. As all the cavities of $Fl(j)$ are obtained as rotations of $U(j)$ we see that vertices of $Fl(j+1)$ differ from vertices of a given cavity of $Fl(j)$ by one of the vectors

$$p_{(\bar{i}, i_{j+1})} - p_{\bar{i}} = K_j \omega(i_{j+1}) + 3 \cdot 4^{-j-1} T_j e_3,$$

$i_{j+1} = 1, 2, 3, 4$. This shows that sets $Fl(j+1, (\bar{i}, i_{j+1}))$ intersect $Fl(j, \bar{i})$ only on the boundaries of its four cavities. Moreover, faces of $Fl(j+1, (\bar{i}, i_{j+1}))$ are faces of certain cavity of $Fl(j, \bar{i})$.

Now we define the mapping

$$u\colon [-\frac{R_1}{2},\frac{R_1}{2}]^2\times[-\frac{1}{2^{\gamma+1}},\frac{1}{2^{\gamma+1}}]\to\mathbf{R}^3$$

such that

$$u|_{Bl_{j,\bar{i}}}(x,y,z)=u_{Bl_{j,\bar{i}}-a_{\bar{i}}}((x,y,z)-a_{\bar{i}})+b_{\bar{i}}.$$

The mapping u is a homeomorphism since all $u|_{Bl_{j,\bar{i}}}$ are and by previous discussions $u|_{Bl_{j,\bar{i}}}$ and $u|_{Bl_{j+1,\bar{i}'}}$ agree on intersections $Bl_{j,\bar{i}}\cap Bl_{j+1,\bar{i}'}$ by Remark 3 since the mappings agree on the vertices in the intersection.

3.5. Properties of u. Now we will show that u is locally Lipschitz continuous outside a small exceptional set and that u fails 2-dimensional Lusin's condition on hyperplane $\mathbf{R}^2\times\{0\}$. To show this we define two more Cantor sets. We set

$$\mathcal{C}_d=\bigcap_{j=1}^{\infty}\bigcup_{\bar{i}\in\mathcal{I}_j}\left(\left[-\frac{R_j}{2},\frac{R_j}{2}\right]^2+a_{\bar{i}}\right)\times\{0\}\subset\mathbf{R}^2\times\{0\}\subset\mathbf{R}^3. \tag{3.27}$$

First notice that by our choice of R_j (3.12) the Hausdorff dimension of $\mathcal{C}_d$ is 0. Every point $x\notin\mathcal{C}_d$ has a neighborhood which intersects only finite number of the sets $Bl(j,\bar{i})$. On each of these sets u is Lipschitz and therefore u is locally Lipschitz outside of $\mathcal{C}_d$.

Moreover, it is easy to see that $\mathcal{C}_d$ is the set of accumulation points of the countable set $\{a_{\bar{i}}\}$. By the definition we have $u(a_{\bar{i}})=p_{\bar{i}}$ for all $\bar{i}$. By continuity the accumulation points of $\{a_{\bar{i}}\}$ are mapped to the accumulation points of $\{p_{\bar{i}}\}$. We will show that the set of accumulation points of $\{p_{\bar{i}}\}$ has positive 2-dimensional Hausdorff measure. First, the z-coordinate of all these accumulation points is

$$z_0=\sum_{j=1}^{\infty}3\cdot 4^{-j-1}T_j.$$

We write $\tilde{p_{\bar{i}}}$ for the projection of $p_{\bar{i}}$ to xy-plane. It is now quite easy to see that the set of accumulation points is

$$\mathcal{C}_t=\bigcap_{j=1}^{\infty}\bigcup_{\{\bar{i}\in\mathcal{I}_j\}}\left([-K_j,K_j]^2+\tilde{p_{\bar{i}}}\right)\times\{z_0\}. \tag{3.28}$$

By (3.7) we have $K_j=2^{-j-3}(1+4^{-j})$ and it is easy to see that

$$\mathcal{H}^2(C_t)=\lim_{j\to\infty}4^j(2K_j)^2>0.$$

Therefore, u fails 2-dimensional Lusin condition on the plane $\mathbf{R}^2\times\{0\}$.

Finally we define $u\colon[-\frac{R_1}{2},\frac{R_1}{2}]^2\times[-\frac{1}{2^{\gamma+1}},\frac{1}{2^{\gamma+1}}]^2\to\mathbf{R}^4$ by

$$u(x,y,z,w)=(u(x,y,z),w). \tag{3.29}$$

By the above discussion this mapping is homeomorphism, locally Lipschitz for all $(x,y,0,w)$ with $(x,y,0)\notin\mathcal{C}_d$ and it fails 2-dimensional Lusin's condition on every plane $\mathbf{R}^2\times\{(0,w)\}$.

4. Final mapping

Our desired mapping

$$F\colon \left[-\frac{R_1}{2}, \frac{R_1}{2}\right]^2 \times [0,1]^2 \to \mathbf{R}^4 \tag{4.1}$$

is

$$F(x,y,z,w) = u \circ \pi \circ S(x,y,z,w). \tag{4.2}$$

As a composition of homeomorphisms this mapping is clearly homeomorphism onto its image.

4.1. *F* is in ACL. We want to show that F is in $W^{1,1}$. It is enough to check that F satisfies ACL-condition and that the derivative is integrable. The ACL-condition means that F is absolutely continuous on $\mathcal{H}^3$-a.e. line parallel to coordinate axes.

We first notice that for every $(x,y) \in \mathbf{R}^2$ we have by the definition of π and S

$$\pi \circ S(\{(x,y)\} \times \mathbf{R}^2) = \{(x,y)\} \times \mathbf{R}^2. \tag{4.3}$$

Recall also that u is locally Lipschitz at every point outside $\mathcal{C}_d \times \mathbf{R}$. Since u is defined on compact set we see that u is, in fact, Lipschitz on every plane parallel to zw-plane which does not intersect the Cantor set $\mathcal{C}_d$.

Let

$$E = \{(x,y,z,w)\colon (x,y,0) \in \mathcal{C}_d\}.$$

By (4.3) we have $\pi \circ S(E) = E$. We have $\mathcal{H}^3(E) = 0$ since the dimension of $\mathcal{C}_d$ is zero (see Subsection 3.5). We denote by E_x the projection to yzw-plane and we define E_y, E_z, E_w similarly. All these projections have also zero $\mathcal{H}^3$-measure.

Consider first the lines parallel to the x-axis. Let $(y,z,w) \notin E_x$. Let

$$L_x = \{(t,y,z,w)\colon\ t \in [t_1,t_2]\}$$

be a line segment contained in the domain. Recall that $\pi \circ S(t,y,z,w) = (t, y, \tilde{\pi} \circ \tilde{S}(z,w))$ and thus $\pi \circ S$ is is just a translation on the line segment and thus Lipschitz. By the definition of E_x we know that $S \circ \pi(L_x)$ does not intersect the E and therefore u is locally Lipschitz on the curve $\pi \circ S(L_x)$. Thus, $F = u \circ \pi \circ S$ is absolutely continuous on this line. Lines parallel to y-axis are handled similarly.

Now consider lines parallel to z-axis. Let $(x_0,y_0,w_0) \notin E_z$ and let

$$L_z = \{(x_0,y_0,t,w_0)\colon\ t \in [t_1,t_2]\}$$

be a line segment. On this line segment $\pi \circ S$ is absolutely continuous. Since $\pi \circ S(E) = E$ and $(x_0,y_0,w_0) \notin E_z$ we have $\operatorname{dist}(\pi \circ S(L_z), E) > 0$. This implies that u is Lipschitz on $\pi \circ S(L_z)$ and absolute continuity of F on L_z now follows. Lines parallel to w-axis are handled analogously. Thus F is absolutely continuous on these lines. This concludes our proof of F being ACL.

4.2. *F* is in $W^{1,2}$. We know that f is continuous and satisfies the ACL-condition. It is now enough to show that $DF \in L^2_{\mathrm{loc}}$.

We will use chain rule to estimate the derivative. In the complement of the set $\left[-\frac{R_1}{2}, \frac{R_1}{2}\right]^2 \times \mathcal{C}_1$ use of chain rule is allowed. To see this notice that u is C^1 outside a set of measure zero, namely the union of the set E (defined in Subsection 4.1) and boundaries of sets $A_{\pm i}$ of all generations of the construction of u. Also mapping S is locally bi-lipschitz outside of $\left[-\frac{R_1}{2}, \frac{R_1}{2}\right]^2 \times \mathcal{C}_1$ and therefore preimages of sets of measure zero have measure zero. Thus, in the complement of $\left[-\frac{R_1}{2}, \frac{R_1}{2}\right]^2 \times \mathcal{C}_1$ we have

$$|DF(\mathbf{x})| \leq |Du(\pi \circ S(\mathbf{x}))|\,|D\pi(S(\mathbf{x}))|\,|DS(\mathbf{x})| \tag{4.4}$$

for almost every $\mathbf{x}$.

In the set $\left[-\frac{R_1}{2}, \frac{R_1}{2}\right]^2 \times \mathcal{C}_1$ the situation is a bit more complex. Notice that u is not differentiable on the set $\left[-\frac{R_1}{2}, \frac{R_1}{2}\right]^2 \times \{0\} \times \mathbf{R}$ as it is defined in different ways on both sides of this plane. Moreover, the preimage of this plane under $\pi \circ S$ contains $\left[-\frac{R_1}{2}, \frac{R_1}{2}\right]^2 \times \mathcal{C}_1$ which has positive 4-dimensional measure. In this case $|Du(\mathbf{y})|$ in (4.4) must be interpreted as the maximum of one-sided partial derivatives of u at $\mathbf{y}$. To show that (4.4) holds almost everywhere with this interpretation of $|Du|$ we consider any point

$$\mathbf{x} = (x, y, z, w) \in \left(\left[-\frac{R_1}{2}, \frac{R_1}{2}\right]^2 \times \mathcal{C}_1\right) \setminus E.$$

The set E is defined in Subsection 4.1. Notice that for such $\mathbf{x}$ we have $\partial_x F(x, y, z, w) = \partial_x u(x, y, \pi \circ S(z, w))$. For $\mathbf{x} \notin E$ this partial derivative exists because even though u is defined in different way on different pieces these definitions agree on the boundaries of pieces. Thus, (4.4) is valid at least when we have $|\partial_x F(x, y, z, w)|$ on the left hand side. Naturally same applies to ∂_y. Now it suffices to show that $\partial_z F(\mathbf{x}) = 0$ and $\partial_w F(\mathbf{x}) = 0$ for $\mathbf{x} \notin E$.

By (4.3) we have $\pi \circ S(E) = E$ and as mentioned in Subsection 4.1 u is locally Lipschitz in the complement of E. Before (2.7) it is stated that S is differentiable and we have $\partial_z S = 0$ and $\partial_w S = 0$. This fact with local Lipschitz continuity of u in the complement of E implies $\partial_z F(\mathbf{x}) = 0$ and $\partial_w F(\mathbf{x}) = 0$ for every $\mathbf{x} \notin E$ as desired.

It follows that

$$\begin{aligned}
&\int_{\left[-\frac{R_1}{2}, \frac{R_1}{2}\right]^2 \times [0,1]^2} |DF(\mathbf{x})|^2 \, d\mathbf{x} = \int_{\left[-\frac{R_1}{2}, \frac{R_1}{2}\right]^2 \times [0,1]^2} |D(u \circ \pi \circ S)(\mathbf{x})|^2 \, d\mathbf{x} \\
&\leq \int_{\left[-\frac{R_1}{2}, \frac{R_1}{2}\right]^2 \times [0,1]^2} |Du(\pi \circ S(\mathbf{x}))|^2 \, |D\pi(S(\mathbf{x}))|^2 \, |DS(\mathbf{x})|^2 \, d\mathbf{x} \\
&\approx \int_{\left[-\frac{R_1}{2}, \frac{R_1}{2}\right]^2 \times [0,1]^2} |Du(\pi \circ S(\mathbf{x}))|^2 \, |DS(\mathbf{x})|^2 \, d\mathbf{x}.
\end{aligned} \tag{4.5}$$

We integrate over the sets $\left[-\frac{R_1}{2}, \frac{R_1}{2}\right]^2 \times \mathcal{C}_1$ and its complement separately.

4.3. Integration over the complement of the Cantor set. On the set

$$\left(\left[-\frac{R_1}{2}, \frac{R_1}{2}\right]^2 \times [0,1]^2\right) \setminus \left(\left[-\frac{R_1}{2}, \frac{R_1}{2}\right]^2 \times \mathcal{C}_1\right)$$

we may use the change of variable since $\pi \circ S$ it belongs to $W^{1,1}$ and satisfies n-dimensional Lusin's condition. This follows from the fact that S is locally Lipschitz outside the set $\left[-\frac{R_1}{2}, \frac{R_1}{2}\right]^2 \times \mathcal{C}_1$.

Biggest issue here is that the derivative and Jacobian of S at a given point $S^{-1} \circ \pi^{-1}(x)$ depend on the distance of x to the set $\mathbf{R}^2 \times \tilde{\pi} \circ \tilde{S}(C_1)$. Therefore it is natural to decompose the domain to tubes around $\mathbf{R}^2 \times \tilde{\pi} \circ \tilde{S}(C_1)$ but our mapping u is defined using 3-dimensional slices. We will decompose the domain into tubes, as mentioned and compute the integral over them first. The total integral is then obtained as a sum over all tubes.

It is easy to see that the Cantor set $\mathcal{C}_3 = \tilde{\pi}(\mathcal{C}_2)$ can be written as $\{0\} \times \mathcal{C}_4$ where $\mathcal{C}_4$ is a one-dimensional Cantor type set. Moreover, we can write this $\mathcal{C}_4$ as

$$\mathcal{C}_4 = \bigcap_{j=1}^{\infty} \bigcup_{I \in \mathcal{I}_j} I_{j,i},$$

where each $\mathcal{I}_j$ consists of 4^j intervals. In fact we can choose these intervals $I_{j,i}$ to be $\tilde{\pi}(Q_{\boldsymbol{v}})$ for $\boldsymbol{v} \in \mathbf{V}^j$ and then they will have all the same size

$$\operatorname{diam}(\tilde{\pi}(Q_{\boldsymbol{v}})) = \tfrac{3}{2} 2^{-\gamma k} 2^{-k}. \tag{4.6}$$

If the parameter γ in definition of $\mathcal{C}_2$ is chosen large enough the sets $2I_{j,i}$, with $i = 1, \dots, 4^j$ are mutually disjoint (see Figure 3).

Define the sets

$$U_{j,i} = \left([-\frac{1}{2}H_j, \frac{1}{2}H_j] \times I_{j,i} \right) \setminus \left(\bigcup_{I \in \mathcal{I}_{j+1},\, I \subset I_{j,i}} [-\frac{1}{2}h_j, \frac{1}{2}h_j] \times I \right).$$

Notice, that for each $(z,w) \in U_{j,i}$ we have $\operatorname{dist}((z,w), \mathcal{C}_3) \approx 2^{-(\gamma+1)j}$ by (3.15), (3.16) and (4.6)

The following lemma says that all the points in $U_{j,i}$ have their preimages under π^{-1} in some squares of our Cantor set construction with the almost the same generation.

Lemma 4.1. *If $(z,w) \in U_{j,i}$, then $\tilde{\pi}^{-1}(z,w) \in \tilde{Q}_v$ with $\boldsymbol{v} \in \mathbf{V}^l$ (see Subsection 2.2 for definitions) with $|l - j| \le k$, where k is independent of j and the chosen point.*

Proof. By assumption we have $d(\mathcal{C}_3, (z,w)) \approx 2^{-(1+\gamma)j}$. Since π is bi-Lipschitz and $\tilde{\pi}(\mathcal{C}_2) = \mathcal{C}_3$ we have

$$C^{-1}L^{-1}2^{-(1+\gamma)j} \le d(\mathcal{C}_2, \tilde{\pi}^{-1}(z,w)) \approx 2^{-(1+\gamma)j} \le CL2^{-(1+\gamma)j},$$

where L is Lipschitz constant of $\tilde{\pi}^{-1}$. This is equivalent to

$$2^{-(1+\gamma)(j-l)} \le d(\mathcal{C}_2, \tilde{\pi}^{-1}(z,w)) \approx 2^{-(1+\gamma)j} \le 2^{-(1+\gamma)(j+l)},$$

which implies the claim. □

Notice that if $\tilde{\pi}^{-1}(z,w)$ is in a square of generation j in construction of $\mathcal{C}_2$ then $S^{-1} \circ \pi^{-1}(z,w)$ is also in a square of generation j, but in the construction of $\mathcal{C}_1$, of course.

This and the previous lemma together with (2.5) and (2.6) imply the following estimates. If $x \in \mathbf{R}^2 \times U_{j,i}$ then we have (up to constants)

$$\left| DS(S^{-1} \circ \pi^{-1}(\mathbf{x})) \right| \lesssim \frac{2^{-cj}}{\varphi(j) - \varphi(j+1)} = 2^{(2-\gamma)j} \tag{4.7}$$

and

$$\left| J_{S^{-1}}(\pi^{-1}(\mathbf{x})) \right| \lesssim 2^{2cj}(\varphi(j) - \varphi(j+1)) = 2^{(2\gamma-2)j}. \tag{4.8}$$

Now we may start the integration. Recall that $I_1=(-1,1)$. Using the change of variable formula, recalling that π is bi-Lipschitz mapping and using (2.9) we obtain

$$
\begin{aligned}
&\int_{\left([-\frac{R_1}{2},\frac{R_1}{2}]^2\times[0,1]^2\right)\setminus\left([-\frac{R_1}{2},\frac{R_1}{2}]^2\times\mathcal{C}_1\right)} |Du(\pi\circ S(\mathbf{x}))|^2\,|DS(\mathbf{x})|^2\,d\mathbf{x}\\
&=\int_{\left(I_1^2\times\tilde\pi\circ\tilde S([0,1]^2)\right)\setminus\left(I_1^2\times\tilde\pi\circ\tilde S(\mathcal{C}_1)\right)} |Du(\mathbf{y})|^2\left|DS(S^{-1}\circ\pi^{-1}(\mathbf{y}))\right|^2 J_{S^{-1}\circ\pi^{-1}}(\mathbf{y})\,d\mathbf{y}\\
&\approx\int_{\left(I_1^2\times\tilde\pi\circ\tilde S([0,1]^2)\right)\setminus\left(I_1^2\times\tilde\pi\circ\tilde S(\mathcal{C}_1)\right)} |Du(\mathbf{y})|^2\left|DS(S^{-1}\circ\pi^{-1}(\mathbf{y}))\right|^2 J_{S^{-1}}(\pi^{-1}(\mathbf{y}))\,d\mathbf{y}\\
&=\sum_{j=1}^{\infty}\sum_{i=1}^{4^j}\int_{I_1^2\times U_{j,i}} |Du(\mathbf{y})|^2\left|DS(S^{-1}\circ\pi^{-1}(\mathbf{y}))\right|^2 J_{S^{-1}}(\pi^{-1}(\mathbf{y}))\,d\mathbf{y}.
\end{aligned}
\tag{4.9}
$$

Using now estimates (4.7) and (4.8) we obtain that

$$
\int_{\left(I_1^2\times[0,1]^2\right)\setminus\left(I_1^2\times\mathcal{C}_1\right)}|Du(\pi\circ S(\mathbf{x}))|^2\,|DS(\mathbf{x})|^2\,d\mathbf{x}\lessapprox\sum_{j=1}^{\infty}\sum_{i=1}^{4^j}4^j\int_{I_1^2\times U_{j,i}}|Du(\mathbf{y})|^2\,d\mathbf{y}.
\tag{4.10}
$$

Applying now Fubini's theorem we obtain

$$
\begin{aligned}
\int_{I_1^2\times U_{j,i}}|Du(\mathbf{y})|^2\,d\mathbf{y}&\le\int_{I_1^2\times[-\frac12 H_j,\frac12 H_j]\times I_{j,i}}|Du(\mathbf{y})|^2\,d\mathbf{y}\\
&\le 2\int_{I_{j,i}}\int_{[0,\frac12 H_j]}\int_{I_1^2}|Du(x,y,z)|^2\,d(x,y)\,dz\,dw\\
&=2\sum_{k=j}^{\infty}\int_{I_{j,i}}\int_{[\frac12 H_{k+1},\frac12 H_k]}\int_{I_1^2}|Du(x,y,z)|^2\,d(x,y)\,dz\,dw.
\end{aligned}
\tag{4.11}
$$

Assume now that $z_0\in[\frac12 H_{k+1},\frac12 H_k]$. We will compute value of

$$
\int_{I_1^2}|Du(x,y,z_0)|^2\,d(x,y).
$$

First, notice that this choice of z_0 means that the hyperplane $\{z=z_0\}$ intersects all blocks $Bl(l,\bar\imath)$, $l\le k$ used in the definition of u (see Subsection 3.4 for definitions). Intersections with $Bl(k,\bar\imath)$ are squares (subsets of A_{+t}) and intersections with $Bl(k,\bar\imath)$ for $l<k$ are rectangular annuli (subsets of A_{+1}, A_{+2}, A_{+3} and A_{+4})—see Figure 6 and (3.1). For this reason we consider these sets separately. That is, we have

$$
\begin{aligned}
\int_{I_1^2}|Du(x,y,z_0)|^2 d(x,y)&=\sum_{l=1}^{k}\sum_{\bar\imath\in\{1,2,3,4\}^l}\int_{B(l,\bar\imath)\cap\{z=z_0\}}|Du(x,y,z)|^2\,d(x,y)\\
&=\sum_{l=1}^{k-1}\sum_{\bar\imath\in\{1,2,3,4\}^l}\underbrace{\int_{\left[-\frac{R_l}{2},\frac{R_l}{2}\right]^2\setminus\left[-\frac{r_l}{2},\frac{r_l}{2}\right]^2+a_{\bar\imath}}|Du(x,y,z_0)|^2\,d(x,y)}_{=:I}\\
&\quad+\sum_{\bar\imath\in\{1,2,3,4\}^k}\underbrace{\int_{\left[-\frac{R_k}{2},\frac{R_k}{2}\right]^2+a_{\bar\imath}}|Du(x,y,z_0)|^2\,d(x,y)}_{=:II}
\end{aligned}
\tag{4.12}
$$

For fixed l these integrals are clearly the same for each $a_{\bar{i}}$. By (3.20) and (3.14) we have for I

$$
\begin{aligned}
I &= \int_{\left[-\frac{R_l}{2},\frac{R_l}{2}\right]^2\setminus\left[-\frac{r_l}{2},\frac{r_l}{2}\right]^2} |Du(x,y,z_0)|^2\, d(x,y) \leq 4\int_{\left[\frac{r_l}{2},\frac{R_l}{2}\right]}\int_{[-x,x]} \frac{4^{-l}}{x^2}\,dy\,dx \\
&= 8\cdot 4^{-l}\int_{\left[\frac{r_l}{2},\frac{R_l}{2}\right]} \frac{1}{x}\,dx = 8\cdot 4^{-l}\log\frac{R_l}{r_l} \leq 8\cdot 4^{-l} l^{\beta}.
\end{aligned}
\tag{4.13}
$$

The case II is similar. However, here we have to take in to account that u is defined differently on the part (subset of A_{+t})

$$
S_k = \left[-\frac{R_k - r_k}{2(H_k - h_k)}(z_0 - \frac{h_k}{2}) + \frac{r_k}{4}, \frac{R_k - r_k}{2(H_k - h_k)}(z_0 - \frac{h_k}{2}) + \frac{r_k}{4}\right]^2
$$

and on the part (subset of $A_{+1}\cup A_{+2}\cup A_{+3}\cup A_{+4}$)

$$
A_k = \left[-\frac{R_k}{2}, \frac{R_k}{2}\right]^2 \setminus S_k.
$$

To simplify notation in the following calculation we denote

$$
D_k(z_0) = \frac{R_k - r_k}{2(H_k - h_k)}(z_0 - \frac{h_k}{2}) + \frac{r_k}{4}.
$$

Using (3.20) and (3.22) we obtain

$$
\begin{aligned}
II &= \int_{\left[-\frac{R_k}{2},\frac{R_k}{2}\right]^2} |Du(x,y,z_0)|^2\, d(x,y) \\
&= \int_{A_k} \left|D\tilde{u}(x,y,z_0)\right|^2\, d(x,y) + \int_{S_k} \left|D\tilde{u}(x,y,z_0)\right|^2\, d(x,y) \\
&\lessapprox 4^{-k}\left[\int_{\left[D_k(z_0),\frac{R_k}{2}\right]}\int_{[-x,x]} \frac{1}{x^2}\,dy\,dx + \int_{[-D_k(z_0),D_k(z_0)]^2} \frac{1}{(D_k(z_0))^2}\,dy\,dx\right] \\
&\lessapprox 4^{-k}\log\frac{R_k}{r_k} \lessapprox 4^{-k}k^{\beta}.
\end{aligned}
\tag{4.14}
$$

Plugging (4.13) and (4.14) into (4.12) we obtain

$$
\int_{I_1^2} |Du(x,y,z_0)|^2\, d(x,y) \leq \sum_{l=1}^{k} 4^l\cdot 4^{-l} l^{\beta} \lessapprox k^{\beta+1}. \tag{4.15}
$$

Inserting this expression into (4.11) and using (3.15) and (4.6) we obtain

$$
\begin{aligned}
\int_{I_1^2\times U_{j,i}} |Du(\mathbf{y})|^2\, d\mathbf{y} &\lessapprox \sum_{k=j}^{\infty}\int_{I_{j,i}}\int_{\left[\frac{1}{2}H_{k+1},\frac{1}{2}H_k\right]} k^{\beta+1} \lessapprox \sum_{k=j}^{\infty} 2^{-2(\gamma+1)k}k^{\beta+1} \\
&\lessapprox 2^{-2(\gamma+1)j} j^{\beta+1}.
\end{aligned}
\tag{4.16}
$$

Finally, (4.10) with (4.16) give

$$
\begin{aligned}
&\int_{\left(I_1^2\times[0,1]^2\right)\setminus\left(I_1^2\times\mathcal{C}_1\right)} |Du(\pi\circ S(\mathbf{x}))|^2\, |DS(\mathbf{x})|^2\, d\mathbf{x} \\
&\lessapprox \sum_{j=1}^{\infty}\sum_{i=1}^{4^j} 4^j \int_{I_1^2\times U_{j,i}} |Du(\mathbf{y})|^2\, d\mathbf{y} \leq \sum_{j=1}^{\infty} 2^{2j-2\gamma j} j^{\beta+1} < \infty
\end{aligned}
\tag{4.17}
$$

here the convergence follows from the choice $\gamma > 1$.

4.4. Integration over the Cantor set. Next we calculate the integral over $\left[-\frac{R_1}{2}, \frac{R_1}{2}\right]^2 \times \mathcal{C}_1$. Notice that in this case we cannot use the change of variable as in previous case. The reason is that $S(I_1^2 \times \mathcal{C}_1)$ is a null set. Remember that by (2.7) we have $DS = 1$. By (3.21) we have

$$|Du(\pi \circ S(x,y,z,w))| = \frac{2^{-j}}{|(x,y) - a_{\bar{i}}|_\infty \log \frac{R_j}{r_j}}$$

for all $(x,y) \in [-\frac{R_j}{2}, \frac{R_j}{2}]^2 \setminus [-\frac{r_j}{2}, \frac{r_j}{2}]^2 + a_{\bar{i}}$ and $(z,w) \in \mathcal{C}_1$.

Using these facts, polar coordinates and (3.14) we obtain

$$\begin{aligned}
&\int_{[-\frac{R_1}{2}\times\frac{R_1}{2}]^2\times\mathcal{C}_1} |Du(\pi\circ S(\mathbf{x}))|^2 \, |DS(\mathbf{x})|^2 \, d\mathbf{x} \\
&= \int_{\mathcal{C}_1}\int_{[-\frac{R_1}{2}\times\frac{R_1}{2}]^2} |Du(\pi\circ S(\mathbf{x}))|^2 \, d\mathbf{x} \\
&= \sum_{j=1}^{\infty} \sum_{\bar{i}\in\{1,2,3,4\}^j} \int_{\mathcal{C}_1}\int_{[-\frac{R_j}{2},\frac{R_j}{2}]^2\setminus[-\frac{r_j}{2},\frac{r_j}{2}]^2+a_{\bar{i}}} |Du(\pi\circ S(\mathbf{x}))|^2 \, d\mathbf{x} \\
&\leq \sum_{j=1}^{\infty} \sum_{\bar{i}\in\{1,2,3,4\}^j} \int_{\mathcal{C}_1}\int_{[-\frac{R_j}{2},\frac{R_j}{2}]^2\setminus[-\frac{r_j}{2},\frac{r_j}{2}]^2} \frac{4^{-j}}{|(x,y)|_\infty^2 \log^2 \frac{R_j}{r_j}} d(x,y)\, d(z,w) \\
&= \mathcal{H}^2(\mathcal{C}_1) \sum_{j=1}^{\infty} \int_{[\frac{r_j}{2},\frac{R_j}{2}]} \frac{1}{r\log^2\frac{R_j}{r_j}} \, dr = \mathcal{H}^2(\mathcal{C}_1)\sum_{j=1}^{\infty}\frac{1}{\log\frac{R_j}{r_j}} \\
&\lessapprox \mathcal{H}^2(\mathcal{C}_1)\sum_{j=1}^{\infty}\frac{1}{j^\beta} < \infty.
\end{aligned} \tag{4.18}$$

Therefore our mapping truly is in $W^{1,2}$ by (4.5), (4.17) and (4.18).

4.5. Failure of Lusin's condition (N) on positively many 2-dimensional hyperplanes. For any $(z,w) \in \mathcal{C}_1$, it suffices to show that F restricted to the hyperplane $\left[-\frac{R_1}{2}, \frac{R_1}{2}\right]^2 \times \{(z,w)\}$ fails to satisfy 2-dimensional Lusin's condition. This is now simple. First, by (2.8)

$$\tilde{\pi} \circ \tilde{S}(\mathcal{C}_1) = \mathcal{C}_3 \subset \{0\} \times \mathbf{R}$$

and, second, u fails 2-dimensional Lusin's condition on every plane $\left[-\frac{R_1}{2}, \frac{R_1}{2}\right] \times \{(0,w)\}$, for which it is defined as was mentioned at the end of Subsection 3.4.

4.6. On higher integrability of the derivative. Let $\Omega \subset \mathbf{R}^k$ and $f \in W^{1,k}(\Omega, \mathbf{R}^k)$. Recall, that the condition

$$|Df|^k \log^\alpha(e + |Df|) \in L^1$$

implies that f satisfies k-dimensional Lusin's (N) condition if $\alpha > 1$ but not necessarily if $\alpha \leq 1$. This follows from more general results in [10].

We can use this result on two-dimensional planes and we obtain that in our example we can't possibly hope better regularity than $L^2 \log L$. Our mapping gets very close to this. One can check that actually $DF \in L^2 \log^\alpha(e+L)$ for every $\alpha < 1$. Mapping does not require real changes, only the choice of β at the end is different. It seems plausible that similar example exists also with $DF \in L^2 \log(e+L)$ but this seems to require a lot of changes in the mapping. Existence of such example would mean that homeomorphicity does not make mapping any better then other Sobolev mappings when one considers 2-dimensional Lusin's condition on planes for mappings between domains in $\mathbf{R}^4$. This is clearly different from the case of codimension 1 by results of [4].

To check the integrability one proceeds as in $W^{1,2}$-case. We list here some differences with the estimates. Integration over the set

$$\left(\left[-\frac{R_1}{2},\frac{R_1}{2}\right]^2\times[0,1]^2\right)\setminus\left(\left[-\frac{R_1}{2},\frac{R_1}{2}\right]^2\times\mathcal{C}_1\right)$$

is essentially the same. Instead of (4.16) one has

$$\begin{aligned}\int_{I_1^2\times U_{j,i}}|Du(\mathbf{y})|^2\log^\alpha(|Du(\mathbf{y})|)\,d\mathbf{y}&\lessapprox\sum_{k=j}^\infty\int_{I_{j,i}}\int_{\left[\frac12 H_{k+1},\frac12 H_k\right]}k^{\beta+1}k^{\alpha\beta}\\&\lessapprox 2^{-2(\gamma+1)j}j^{\beta(\alpha+1)+1}\end{aligned}\tag{4.19}$$

but this does not affect the convergence of the integral analogous to (4.17).

The integration over the Cantor set is similar. Instead of (4.18) we have

$$\begin{aligned}&\int_{\left[-\frac{R_1}{2}\times\frac{R_1}{2}\right]^2\times\mathcal{C}_1}|Du(\pi\circ S(\mathbf{x}))|^2\,|DS(\mathbf{x})|^2\log^\alpha(e+|Du(\pi\circ S(\mathbf{x}))|)\,d\mathbf{x}\\&\lessapprox\mathcal{H}^2(\mathcal{C}_1)\sum_{j=1}^\infty\frac{\log^\alpha\frac{1}{r_j}}{\log\frac{R_j}{r_j}}\lessapprox\mathcal{H}^2(\mathcal{C}_1)\sum_{j=1}^\infty\frac{j^{\alpha(\beta+1)}}{j^\beta}<\infty\end{aligned}\tag{4.20}$$

for β big enough as $\alpha<1$ is fixed. These two estimates give the desired integrability.

Acknowledgement. The authors would like to thank to Marcos de la Oliva and Changyu Guo for pointing their interest to the problem. The authors would also like to thank to the referee for carefully reading the manuscript.

References

[1] Ball, J.: Global invertibility of Sobolev functions and the interpenetration of matter. - Proc. Roy. Soc. Edinburgh Sect. A 88, 1981, 315–328.

[2] Cesari, L.: Sulle transformazioni continue. - Ann. Math. Pura Appl. 21, 1942, 157–188.

[3] Campbell, D., S. Hencl, and V. Tengvall: Approximation of $W^{1,p}$ Sobolev homeomorphism by diffeomorphisms and the signs of the Jacobian. Preprint, MATH-KMA-2016/522, 2016.

[4] Csörnyei, M., S. Hencl, and J. Malý: Homeomorphisms in the Sobolev space $W^{1,n-1}$. - J. Reine Angew. Math. 644, 2010, 221–235.

[5] Faraco, D., C. Mora-Corral, and M. Oliva: Sobolev homeomorphisms with gradients of low rank via laminates. - Adv. Calc. Var. (to appear).

[6] Hajłasz, P.: Change of variables formula under minimal assumptions. - Colloq. Math. 64, 1993, 93–101.

[7] Hencl, S., and P. Koskela: Lectures on mappings of finite distortion. - Lecture Notes in Math. 2096, Springer, 2014.

[8] Iwaniec, T., and G. Martin: Geometric function theory and nonlinear analysis. - Oxford Math. Monogr., Clarendon Press, Oxford, 2001.

[9] Kauhanen, J., P. Koskela, and J. Malý: Mappings of finite distortion: Condition N. - Michigan Math. J. 49, 2001, 169–181.

[10] Kauhanen, J., P. Koskela, and J. Malý: On functions with derivatives in a Lorentz space. Manuscripta Math. 100:1, 1999, 87–101.

[11] Malý, J., and O. Martio; Lusin's condition (N) and mappings of the class $W^{1,n}$. - J. Reine Angew. Math. 458, 1995, 19–36.

[12] Malý, J., D. Swanson, and W. P. Ziemer: Coarea formula for Sobolev mappings. - Trans. Amer. Math. Soc. 355:2, 2003, 477–492.

[13] Oliva, M.: Bi-Sobolev homeomorphisms f with Df and Df^{-1} of low rank using laminates. - Calc. Var. Partial Differential Equations 55:6, 2016, article 135.

[14] Ponomarev, S.: Examples of homeomorphisms in the class $ACTL^p$ which do not satisfy the absolute continuity condition of Banach. - Dokl. Akad. Nauk USSR 201, 1971, 1053–1054 (in Russian).

[15] Reshetnyak, Yu. G.: Some geometrical properties of functions and mappings with generalized derivatives. - Sibirsk. Math. Zh. 7, 1966, 886–919.

[16] Ziemer, W. P.: Weakly differentiable function: Sobolev spaces and functions of bounded variation. - Grad. Texts in Math. 120, Springer-Verlag, New York, 1989.

Received 3 November 2016 • Accepted 23 December 2016